



UNIVERSIDADE FEDERAL DE UBERLÂNDIA

INSTITUTO DE CIÊNCIAS BIOMÉDICAS

PROGRAMA DE PÓS-GRADUAÇÃO EM IMUNOLOGIA E PARASITOLOGIA
APLICADAS



**ATIVIDADE ANTIVIRAL DE TOXINAS DE SERPENTE *BOTHROPS*
JARARACUSSU NO CICLO REPLICATIVO DO ZIKA VÍRUS**

NATASHA MARQUES CASSANI

UBERLÂNDIA

Junho – 2022

UNIVERSIDADE FEDERAL DE UBERLÂNDIA
INSTITUTO DE CIÊNCIAS BIOMÉDICAS
PROGRAMA DE PÓS-GRADUAÇÃO EM IMUNOLOGIA E PARASITOLOGIA
APLICADAS

**ATIVIDADE ANTIVIRAL DE TOXINAS DE SERPENTE *BOTHRUPS*
JARARACUSSU NO CICLO REPLICATIVO DO ZIKA VÍRUS**

NATASHA MARQUES CASSANI

Dissertação apresentada ao
colegiado do Programa de Pós-
Graduação em Imunologia e
Parasitologia Aplicadas como
requisito parcial para obtenção
do título de mestre.

Orientadora: Profa. Dra. Ana
Carolina Gomes Jardim

UBERLÂNDIA

Junho – 2022

Ficha Catalográfica Online do Sistema de Bibliotecas da UFU com dados informados pelo (a) próprio (a) autor(a).

C343 Cassani, Natasha Marques, 1997-
2022 ATIVIDADE ANTIVIRAL DE TOXINAS DE SERPENTE
BOTHROPS JARARACUSSU NO CICLO REPLICATIVO DO
ZIKA VÍRUS [recurso eletrônico] / Natasha Marques Cassani. -
2022.

Orientadora: Ana Carolina Gomes Jardim.
Dissertação (Mestrado) - Universidade
Federal de
Uberlândia, Pós-graduação em Imunologia e
Parasitologia Aplicadas.

Modo de acesso: Internet.

Disponível em:

<http://doi.org/10.14393/ufu.di.2022.327>Inclui
bibliografia.

Inclui ilustrações.

1. Imunologia. I. Jardim, Ana Carolina
Gomes, 1981-, (Orient.). II. Universidade Federal de
Uberlândia. Pós-graduação em Imunologia e
Parasitologia Aplicadas. III. Título.

Bibliotecários responsáveis pela estrutura de acordo com o
AACR2: Gizele Cristine Nunes do Couto - CRB6/2091
Nelson Marcos Ferreira - CRB6/307



UNIVERSIDADE FEDERAL DE UBERLÂNDIA
 Coordenação do Programa de Pós-Graduação em Imunologia e Parasitologia
 Aplicada

Av. Amazonas, s/n, Bloco 4C, Sala 4C218 - Bairro Umuarama, Uberlândia-MG, CEP 38400-902
 Telefone: (34) 3225-8672 - www.imunoparasito.ufu.br - coipa@ufu.br



ATA DE DEFESA - PÓS-GRADUAÇÃO

Programa de Pós-Graduação em:	Imunologia e Parasitologia Aplicadas				
Defesa de:	Dissertação de Mestrado nº 279				
Data:	trinta de junho de dois mil e vinte dois	Hora de início:	13:30	Hora de encerramento:	17:05
Matrícula do Discente:	12022IPA004				
Nome do Discente:	Natasha Marques Cassani				
Título do Trabalho:	Atividade antiviral de toxinas de serpente bothrops jararacussu no ciclo replicativo do zika vírus				
Área de concentração:	Imunologia e Parasitologia Aplicadas				
Linha de pesquisa:	Biologia das interações entre patógenos e seus hospedeiros				
Projeto de Pesquisa de vinculação:	Rede de pesquisa em doenças infecciosas humanas e animais no estado de Minas Gerais				

Reuniu-se no dia 30 de junho, as 13:30 horas, por vídeo conferência, a Banca Examinadora designada pelo Colegiado do Programa de Pós-graduação em Imunologia e Parasitologia Aplicadas, assim composta pelos titulares: Pedro Paulo Corbi - UNICAMP; Marcos Batista Machado - UFAM; Ana Carolina Gomes Jardim - (Presidente) orientadora da candidata.

Iniciando os trabalhos o (a) presidente da mesa, Profa. Dra. Ana Carolina Gomes Jardim apresentou a Comissão Examinadora, e o candidato(a), agradeceu a presença do público, e concedeu a Discente a palavra para a exposição do seu trabalho. A duração da apresentação da Discente e o tempo de arguição e resposta foram conforme as normas do Programa.

A seguir o senhor(a) presidente concedeu a palavra, pela ordem sucessivamente, aos(às) examinadores(as), que passaram a arguir o(a) candidato(a). Ultimada a arguição, que se desenvolveu dentro dos termos regimentais, a Banca, em sessão secreta, atribuiu o resultado final, considerando o(a) candidato(a):

APROVADA.

Esta defesa faz parte dos requisitos necessários à obtenção do título de Mestre.

O competente diploma será expedido após cumprimento dos demais requisitos, conforme as normas do Programa, a legislação pertinente e a regulamentação interna da UFU.

Nada mais havendo a tratar foram encerrados os trabalhos. Foi lavrada a presente ata que após lida e achada conforme foi assinada pela Banca Examinadora.



Documento assinado eletronicamente por **Ana Carolina Gomes Jardim, Professor(a) do Magistério Superior**, em 30/06/2022, às 17:05, conforme horário oficial de Brasília, com fundamento no art. 6º, § 1º, do [Decreto nº 8.539, de 8 de outubro de 2015](#).

Documento assinado eletronicamente por **Pedro Paulo Corbi, Usuário Externo**, em 30/06/2022, às



17:06, conforme horário oficial de Brasília, com fundamento no art. 6º, § 1º, do [Decreto nº 8.539, de 8 de outubro de 2015](#).



Documento assinado eletronicamente por **Marcos Batista Machado, Usuário Externo**, em 30/06/2022, às 17:06, conforme horário oficial de Brasília, com fundamento no art. 6º, § 1º, do [Decreto nº 8.539, de 8 de outubro de 2015](#).



A autenticidade deste documento pode ser conferida no site https://www.sei.ufu.br/sei/controlador_externo.php?acao=documento_conferir&id_orgao_acesso_externo=0, informando o código verificador **3699697** e o código CRC **087BF4E0**.

AGRADECIMENTOS

Meus sinceros agradecimentos, primeiramente à minha orientadora, a quem devo a realização deste trabalho. Obrigada por toda a ajuda, orientação, carinho e principalmente paciência. Seus ensinamentos são essenciais para minha trajetória.

Aos meus pais e à minha irmã, a quem devo minha trajetória. Obrigada por tudo o que fizeram e fazem por mim, vocês são a razão dos meus esforços e das minhas vitórias, especialmente a do momento presente.

Ao meu companheiro, a quem devo meu presente. Obrigada por ser o maior incentivador de tudo o que realizo. Seu apoio é essencial para todos os momentos e aprendizados felizes que tenho.

Aos meus amigos de laboratório, a quem devo meus aprendizados. Vocês me ensinam em absolutamente todos os momentos. A estrada não teria sido tão leve e feliz sem a presença de vocês.

E à Deus, pela estrada que percorri até aqui. Obrigada!

*“Quando ouvi o astrônomo erudito,
Quando as provas, os números, foram listados em colunas diante de mim,
Quando me foram apresentados os mapas e diagramas, para somar, dividir e medi-los,
Quando eu, sentado, ouvi o astrônomo no auditório em que apresentava sua palestra com
grande aplauso,
Bem cedo e sem conta me senti cansado e enojado,
Até que, levantando-me e saindo silenciosamente, fui perambular na solidão,
No místico ar úmido da noite e, de tempo em tempo,
Mirava no céu a perfeição silenciosa das estrelas.”*
(Walt Whitman)

LISTA DE ABREVIATURAS E SIGLAS

Asp	Aspartato
AXL	Receptor tirosina quinase
BHE	Barreira hematoencefálica
BTHTX-I	Bothropstoxina I de <i>Bothrops jararacussu</i>
BTHTX-II	Bothropstoxina II de <i>Bothrops jararacussu</i>
C	Proteína do capsídeo viral
DC-SIGN	Receptor de lectina
DENV	Vírus da Dengue
DMEM	Dulbecco's Modified Eagle Medium (Meio básico modificado por Dulbecco)
DMSO	Dimetilsulfóxido
E	Proteína do envelope viral
ECA	Enzima Conversora de Angiotensina
GBS	<i>Guillain-Barré Syndrome</i> (Síndrome de Guillain-Barré)
His	Histidina
HIV	Vírus da Imunodeficiência Humana
HCV	Hepacivírus C
Lys	Lisina
M	Protéina de membrana
MOI	<i>Multiplicity of infection</i> (Multiplicidade de infecção)
MTT	3-(4,5-dimethylthiazol-2-yl)-2,5-diphenyltetrazolium-bromide (Brometo de 3-(4',5'-dimetiltiazol-2'-ila)-2,5-difeniltetrazol)
nsP	<i>Non-structural proteins</i> (Proteínas não estruturais)
OMS	Organização Mundial da Saúde
ORFs	<i>Open Reading Frame</i> (Regiões de leitura aberta)
PLA₂	Fosfolipase A ₂
pH	Potencial hidrogênico
RE	Retículo endoplasmático
RNA	Ribonucleicacid (Ácido ribonucleico)
Rdrp	RNA polimerase dependente de RNA
TAM	Receptor tirosina quinase
TIM-1	Receptor tirosina quinase
YFV	Vírus da Febre Amarela

ZIKV

Vírus da Zika

LISTA DE FIGURAS

Figura 1: Taxa de incidência do ZIKV no Brasil. Regiões do país que registraram casos de Zika até a SE 19 de 2022, de acordo com o Boletim Epidemiológico do Ministério da Saúde (MS).	14
Figura 2: Estrutura da partícula viral e genoma do ZIKV: Esquema representativo da partícula viral do ZIKV (PDB: 5JHM) (A). Ilustração do genoma do ZIKV (B).	15
Figura 3: Esquema representativo do ciclo replicativo do ZIKV.	16
Figura 4: Sintomas frequentemente associados à Febre Zika.	17
Figura 5: Esquema ilustrativo da microcefalia.	19
Figura 6: Estrutura das bothropstoxinas I e II isoladas da peçonha de Bothrops jararacussu. BthTX-I (PDB: 3HZD) (A). BthTX-II (PDB: 2OQD) (B).....	22

RESUMO

Zika vírus (ZIKV) é o agente etiológico da febre Zika, uma infecção transmitida por mosquitos, de disseminação global, e previamente associada a casos de microcefalia. Potenciais novos surtos por ZIKV são problemas prioritários para os órgãos governamentais, visto que as arboviroses são infecções facilmente disseminadas em regiões tropicais como o Brasil. De acordo com o Ministério da Saúde, o ZIKV representa um problema de saúde pública mundial, resultando em impactos social, econômico e no sistema público de saúde (SUS) significativos, uma vez que não há tratamento antiviral eficaz ou vacinas licenciadas. Nesse contexto, compostos naturais apresentam diversas atividades biológicas reportadas, como antioxidante, antiparasitária, antibacteriana e antiviral, bem com toxinas isoladas de serpentes têm demonstrado atividade contra diversos vírus. Neste trabalho, a atividade anti-ZIKV das Bothropstoxinas-I e II (BthTX-I e II) isoladas do veneno de *Bothrops jararacussu* foi investigada contra o ZIKV *in vitro*. Células Vero E6 foram infectadas com ZIKV_{PE243} na presença dos compostos por 72 horas, quando os focos de infecção foram quantificados. Os resultados demonstraram que BthTX-I e II apresentaram potente inibição dose-dependente da infecção pelo ZIKV, com índice de seletividade de 149,1 e $1,44 \times 10^5$, respectivamente. Essas toxinas inibiram principalmente os estágios iniciais do ciclo replicativo do vírus, como a entrada do ZIKV nas células hospedeiras, demonstrado pelo potente efeito virucida, sugerindo a ação dessas toxinas sobre as partículas virais. Adicionalmente, BthTX-I e II apresentaram atividade significativa nos estágios tardios do ciclo replicativo do ZIKV. Análises de *docking* molecular mostraram que BthTX-I e II potencialmente interagem com a proteína do Envelope do ZIKV através de ligações de hidrogênio e interações hidrofóbicas. Nossos dados demonstram que essas toxinas podem ser usadas como modelos úteis para o desenvolvimento de futuros antivirais contra a febre Zika.

Palavras-chave: antiviral, Zika vírus, toxinas.

ABSTRACT

Zika virus (ZIKV) is the etiologic agent of Zika fever, a globally spreading mosquito-borne infection, previously associated with cases of microcephaly. Potential new outbreaks of ZIKV are priority problems for the governments since arboviruses are infections that are easily spread in tropical regions such as Brazil. According to the Ministry of Health, ZIKV represents a worldwide public health problem, resulting in social, economic, and public health system (SUS) significant impacts, since there is no effective antiviral treatment and licensed vaccines. In this context, natural compounds have several biological reported activities, such as antioxidant, antiparasitic, antibacterial, and antiviral, as well as toxins isolated from the venom of snakes have shown activity against several viruses. Here the anti-ZIKV activity of Bothropstoxins-I and II (BthTX-I and II) isolated from *Bothrops jararacussu* venom was investigated. Vero E6 cells were infected with ZIKV_{PE243} in the presence of compounds for 72 hours, when virus titers were quantified. The results demonstrated that BthTX-I and II presented strong dose-dependent inhibition, with a selective index of 149.1 and 1.44×10^5 , respectively. These toxins mainly inhibited the early stages of the replicative cycle, such as during the entry of ZIKV into host cells, as shown by the potent virucidal effect, suggesting the action of these toxins on the virus particles. Moreover, BthTX-I and II presented significant activity towards the post-entry stages of the ZIKV replicative cycle. Molecular docking analyses showed that BthTX-I and II potentially interact with ZIKV Envelope protein through hydrogen bonds and hydrophobic interactions. Our findings show that these toxins could be used as useful templates for the development of future antiviral candidate drugs against Zika fever.

Keywords: antiviral, Zika virus, toxins.

SUMÁRIO

CAPÍTULO I – FUNDAMENTAÇÃO TEÓRICA.....	12
INTRODUÇÃO.....	13
Histórico e Epidemiologia da Febre Zika.....	13
Zika vírus.....	14
Febre Zika.....	16
Tratamento da Febre Zika.....	18
Compostos naturais e as toxinas de animais.....	18
Bothropstoxinas I e II de <i>Bothrops jararacussu</i>	19
OBJETIVOS.....	21
Objetivos específicos.....	21
REFERÊNCIAS.....	22
CAPÍTULO II.....	33
ROLES OF BOTHROPS JARARACUSSU TOXINS I AND II: ANTIVIRAL FINDINGS AGAINST ZIKA VIRUS.....	30
CAPÍTULO III	57
<i>Considerações finais</i>	58

CAPÍTULO I

Fundamentação Teórica

INTRODUÇÃO

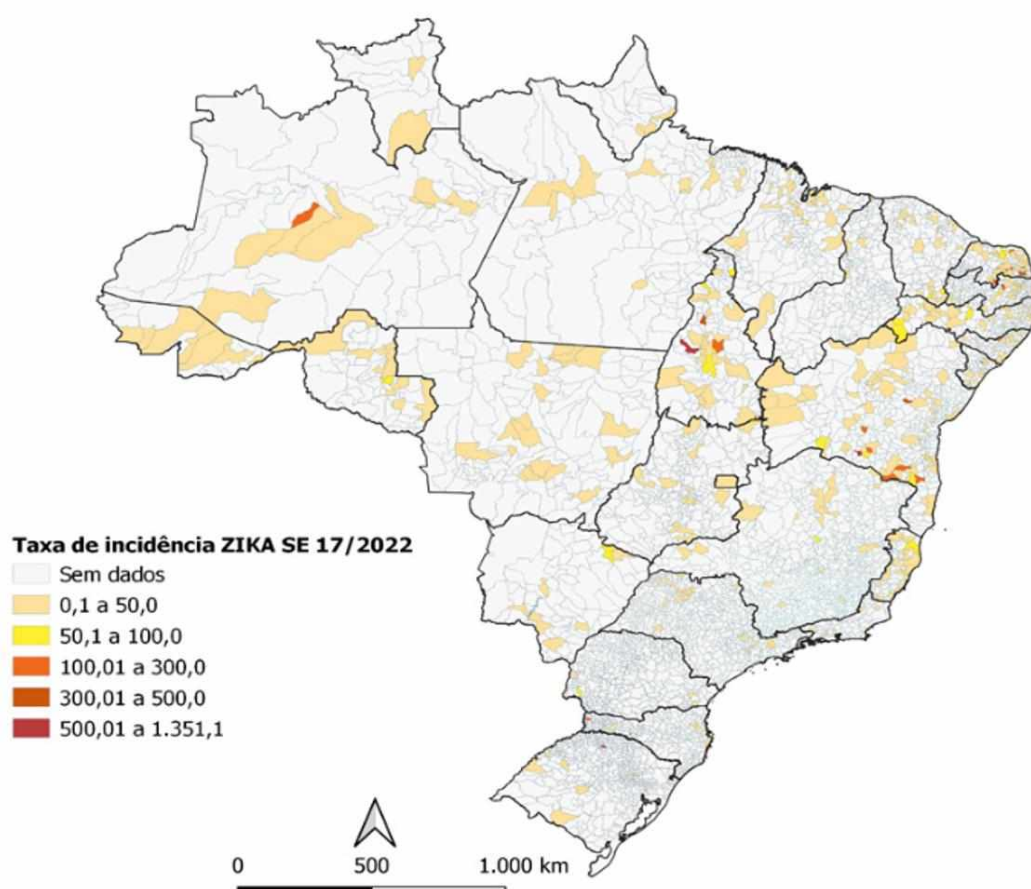
História e Epidemiologia da Febre Zika

O Zika vírus (ZIKV) foi isolado pela primeira vez em macacos, em Uganda, 1947 (DICK, et al 1952). O primeiro caso em humanos de Febre Zika, doença causada pelo ZIKV, foi reportado em uma criança na Nigéria em 1952 (MACNAMARA, 1954). Posteriormente, no ano de 2007, a identificação de casos esporádicos em Yap, ilha da Federação dos Estados da Micronésia e no leste da Polinésia, marcou o início da disseminação do ZIKV para diferentes regiões do mundo (DUFFY et al., 2009; LANCIOTTI et al., 2008). Em 2013, novos casos foram confirmados em outras regiões, como no sul da Ásia, em países como Tailândia (TAPPE et al., 2014), Cambodia (HEANG et al., 2012), Malásia (TAPPE et al., 2015) e Indonésia (KWONG; DRUCE; LEDER, 2013). O ZIKV foi detectado pela primeira vez nas Américas em 2015 (MARINI et al., 2017; FELLNER, 2016; SUMMERS; ACOSTA; ACOSTA, 2015).

No Brasil, os primeiros casos autóctones de ZIKV foram detectados em 2015 na região Nordeste do país (CARDOSO et al., 2015; CAMPOS; BANDEIRA; SARDI, 2015; ZANLUCA et al., 2015). Ao final do ano, casos de infecção por ZIKV já haviam sido detectados em 14 estados brasileiros (WHO, 2015), com uma estimativa de 440.000 a 1.300.000 casos suspeitos (HENNESSEY; FISCHER; STAPLES, 2016). Em março de 2016, o país apresentava 51.473 casos confirmados, além de relatos da infecção em 48 países das Américas. Com o aumento expressivo de casos nas Américas, a Organização Mundial de Saúde (OMS) declarou a Febre Zika como uma “emergência de saúde pública de interesse internacional” em 2016 (WHO, 2016).

De acordo com o último boletim epidemiológico no Brasil, em 2022 foram notificados 3.140 casos prováveis de ZIKV até a semana epidemiológica (SE) 19 (taxa de incidência de 1,5 caso/100 mil habitantes), com maior taxa de incidência nas regiões Norte e Nordeste e aumento de 70,7% em relação ao ano de 2021 (MS, 2022) (**Figura 1**). De acordo com a OMS, pelo menos 87 países e territórios já reportaram casos autóctones de infecção pelo ZIKV, com potencial para reemergência do vírus (WHO, 2019).

Figura 1: Taxa de incidência do ZIKV no Brasil. Regiões do país que registraram casos de Zika até a SE 19 de 2022, de acordo com o Boletim Epidemiológico do Ministério da Saúde (MS).



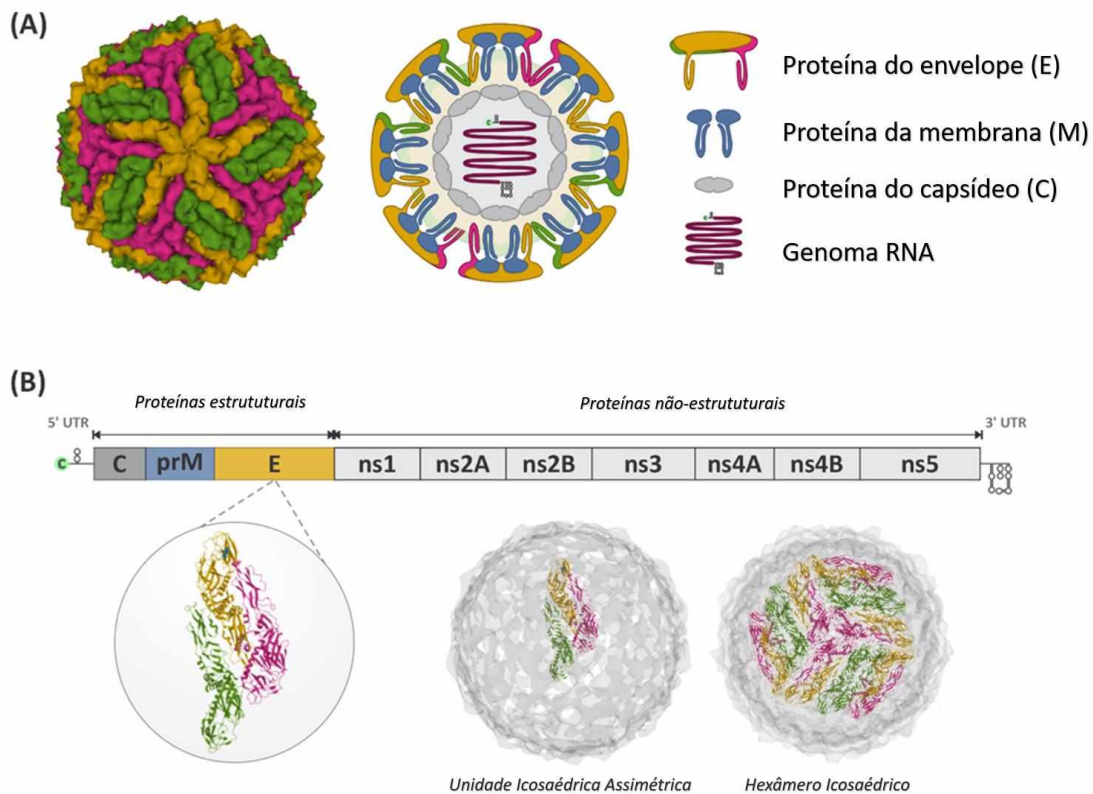
Adaptado de (“Boletim Epidemiológico – Monitoramento dos casos de arboviroses até a semana epidemiológica 19 de 2022, MS, 2022”).

Partícula Viral e Ciclo Replicativo

O ZIKV pertence ao gênero *Flavivirus*, família *Flaviviridae* (MASMEJAN et al., 2020), e é caracterizado por uma partícula viral de 40-60 nm de diâmetro, com capsídeo icosaédrico e um envelope lipídico derivado das membranas da célula hospedeira, onde estão inseridas as proteínas de Envelope (E) (JAVED et al., 2018) (**Figura 2A**). Seu genoma é constituído de uma fita de RNA simples de polaridade positiva com 11.000 pares de bases, que codificam aproximadamente 3.500 aminoácidos (SHARMA et al., 2020; COX; STANTON; SCHINAZI, 2015) (**Figura 2B**). Contém um “cap” na região 5’ UTR (“untranslated region”, região não traduzida) e uma cauda poli-A na 3’ UTR, sendo o domínio DI da 5’ UTR responsável por promover a atividade da RNA polimerase dependente de RNA (RdRp) (BUJALOWSKI;

BUJALOWSKI; CHOI, 2017). Possui apenas uma ORF (“open reading frame”, região aberta de leitura), que codifica uma poliproteína precursora, a qual é clivada em três proteínas estruturais (capsídeo (C), envelope (E) e membrana (prM)) e sete proteínas não estruturais (NS1, NS2A, NS2B, NS3, NS4A, NS4B e NS5) (BOS et al., 2019) (Figura 2B).

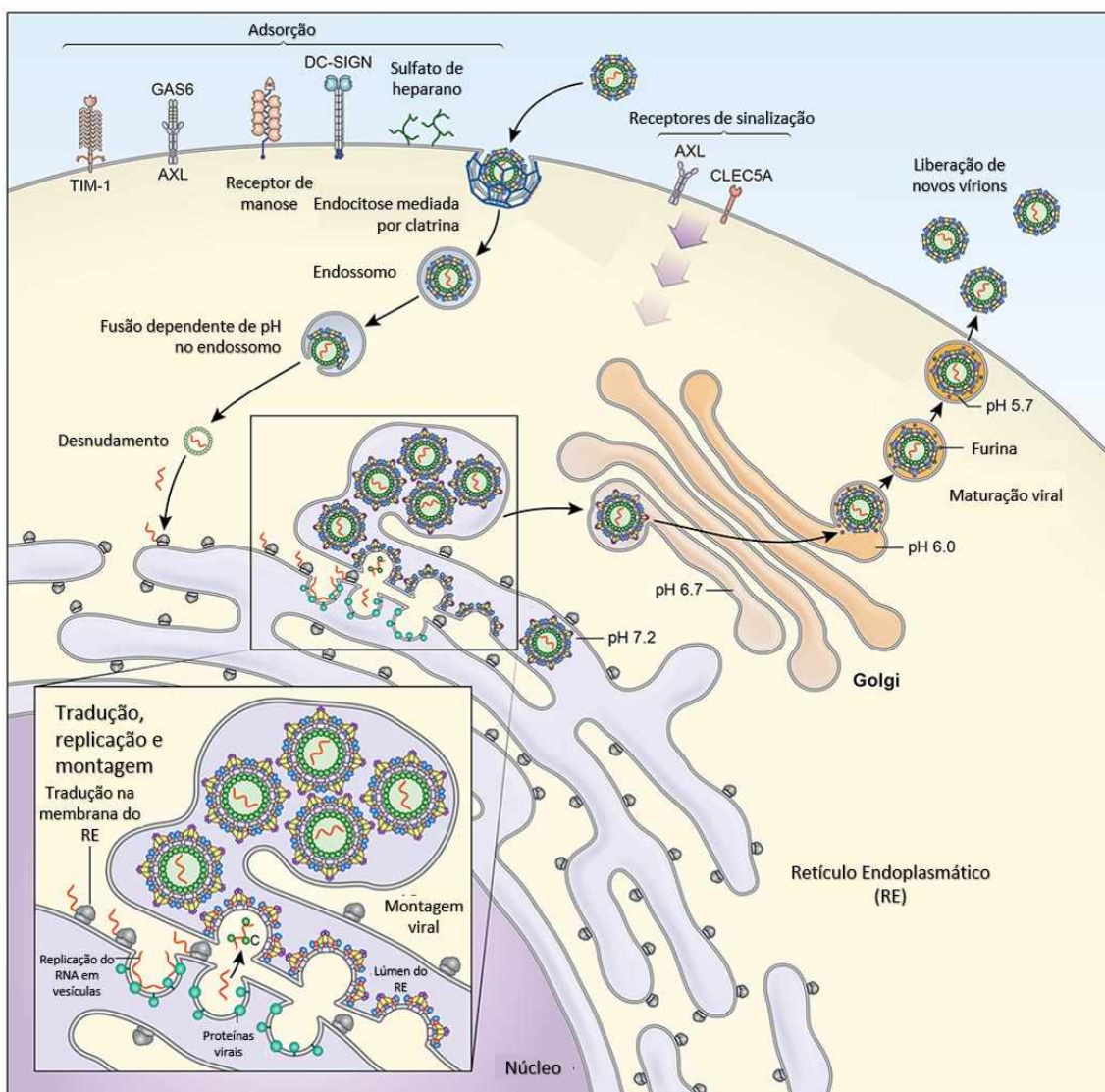
Figura 2: Estrutura da partícula viral e genoma do ZIKV: Esquema representativo da partícula viral do ZIKV (PDB: 5JHM) (A). Ilustração do genoma do ZIKV (B).



O ciclo replicativo do vírus se divide entre células de hospedeiros vertebrados e de artrópodes, sendo assim classificada como uma arbovirose (ROIZ et al., 2018). A replicação viral no hospedeiro vertebrado se inicia pela ligação da glicoproteína E do envelope viral aos receptores da membrana da célula, incluindo os receptores tirosina quinase (TAM - AXL e TIM-1), receptores de manose, receptores de lectina (DC-SIGN) e sulfatos de heparano na superfície celular (PIERSON; DIAMOND, 2020; MA; YUAN; YI, 2022). A internalização da partícula viral ocorre principalmente por meio de endocitose mediada por clatrina, permitindo a formação do endossomo (HACKETT; CHERRY, 2018). O lúmen endossômico contendo o ZIKV torna-se ácido, ativando glicoproteínas de superfície a sofrer alterações conformacionais, induzindo à fusão das

glicoproteínas E com a membrana endossomal, e liberando o capsídeo e o RNA viral no citoplasma [2–5]. O genoma de RNA de fita simples e sentido positivo é então transportado para o retículo endoplasmático (RE) (MOHD ROPIDI et al., 2020), onde é rapidamente traduzido em uma poliproteína precursora, que, após clivada por proteases virais e celulares, gera as três proteínas estruturais necessárias para a formação de vírions infecciosos, e as sete proteínas não estruturais essenciais para a replicação do RNA genômico viral (MOHD ROPIDI et al., 2020). Desta forma, forma-se o complexo replicativo que catalisará a síntese de uma fita de RNA de polaridade negativa, que servirá de molde para sintetizar novas fitas com polaridade positiva. Por fim, ocorre a montagem dos componentes virais e as novas partículas virais são liberadas por exocitose (DIOSA-TORO et al., 2020) (Figura 3).

Figura 3: Esquema representativo do ciclo replicativo do ZIKV.

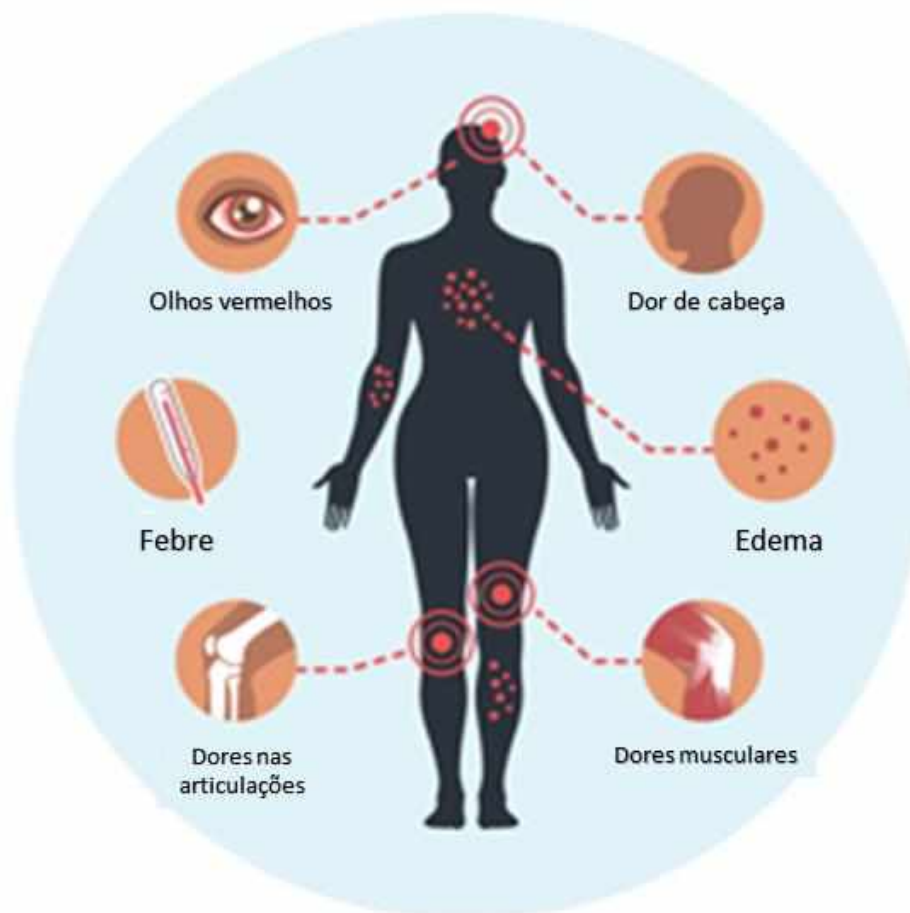


Adaptado de [1].

Febre Zika

A febre Zika é uma doença viral geralmente caracterizada por sintomas leves, que podem durar até 7 dias. Os principais sintomas são comuns aos de outras arboviroses e incluem febre, dores de cabeça, mal-estar, dores no corpo, edema e dores nas articulações (PIELNAA et al., 2020) (**Figura 4**).

Figura 4: Sintomas frequentemente associados à Febre Zika.



Adaptado de (“Zika Virus | Symptoms | CDC, 2019”)

Diferentemente de outras arboviroses, a infecção pelo ZIKV foi correlacionada ao aumento expressivo no número de casos de neonatos com más formações congênitas, atualmente denominada de Síndrome Congênita associada ao Zika (SCHULER-FACCINI et al., 2016; PIERSON; DIAMOND, 2020), fato que resultou em aproximadamente 4000 casos de microcefalia, confirmados pela presença de partículas

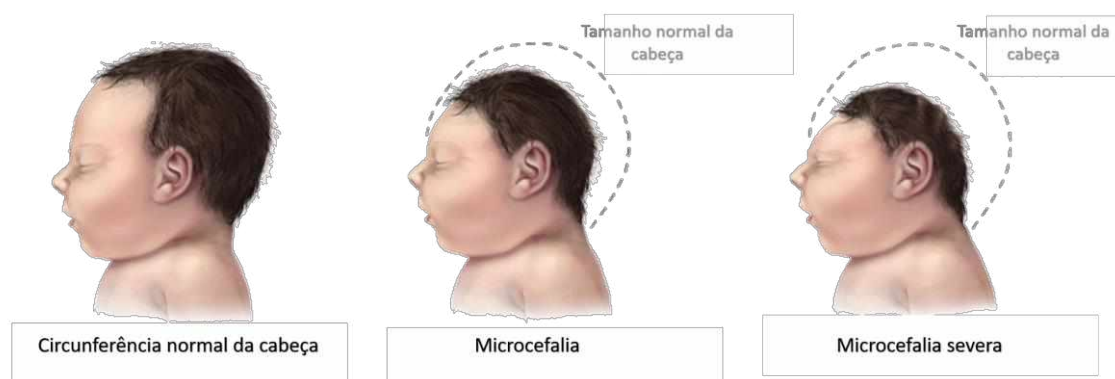
virais do ZIKV no líquido amniótico de gestantes infectadas, e em vários tecidos de fetos com microcefalia (BRASIL et al., 2016; CALVET et al., 2016; MLAKAR et al., 2016; SARNO et al., 2016; SCHULER-FACCINI et al., 2016; VICTORA et al., 2016).

A transmissão do ZIKV ocorre a partir da picada de mosquitos fêmeas do gênero *Aedes*, sendo as principais espécies transmissoras o *Aedes aegypti* e o *Aedes albopictus* (MASMEJAN et al., 2020). Entretanto, trabalhos na literatura mostraram que também podem haver outras formas de transmissão, como a transmissão por contato sexual (FOY et al., 2011), transmissão vertical (BESNARD et al., 2014) e transfusão sanguínea (MAGNUS et al., 2018).

Após a picada do mosquito, o ZIKV é liberado na derme e na corrente sanguínea do hospedeiro vertebrado, inicialmente infectando células suscetíveis ao vírus como as do tecido conjuntivo, fibroblastos, queratinócitos e células dendríticas, mediado pelos receptores TAM [2]. Entretanto, o vírus pode ser transmitido verticalmente e é capaz de atravessar a barreira placentária, infectando macrófagos e citotrofoblastos da placenta. Dessa forma, ele é capaz de infectar o feto em desenvolvimento e conseqüentemente seu sistema nervoso, visto que ele apresenta um tropismo por células progenitoras neurais (CHRISTIAN; SONG; MING, 2019). Essas células expressam receptor AXL, o que leva à degradação de junções aderentes, redução da proliferação celular e conseqüentemente apoptose, mecanismos similares à microcefalia genética (CHRISTIAN; SONG; MING, 2019). Crianças nascidas com microcefalia apresentam uma circunferência do crânio reduzida, devido à má formação neuronal, condição esta que leva à incapacidade motora, sensorial e cognitiva, por toda a sua vida (MLAKAR et al., 2016) **(Figura 5)**.

Adicionalmente, a patologia é associada ao desenvolvimento da síndrome de Guillain-Barré (GBS) em adultos, após o acometimento da febre Zika (CAO-LORMEAU et al., 2016; ROZÉ et al., 2016; OEHLER et al., 2014). GBS é um distúrbio neurológico, caracterizado como doença autoimune, que afeta principalmente adultos acima de 30 anos. Os sintomas estão relacionados à desordem motora e perda sensorial dos músculos faciais e respiratórios (CAO-LORMEAU et al., 2016). Neste caso, o vírus atravessa a barreira hematoencefálica (BHE) e infecta células da glia e oligodendrócitos, destruindo a bainha de mielina e levando as células à apoptose (VOLPI et al., 2018).

Figura 5: Esquema ilustrativo da microcefalia.



Adaptado de (“Zika Virus | Microcephaly & Other Birth Defects | CDC, 2020”)

Profilaxia e Tratamento da Febre Zika

A profilaxia da Febre Zika inclui o controle de vetores e proteção individual. O uso de repelentes, inseticidas e mosquiteiros minimizam a exposição aos vetores [6,7]. O cuidado com água parada impede a proliferação dos mosquitos. Além disso, a OMS recomenda a prática de proteção sexual, principalmente para mulheres gestantes que vivem em áreas de alta transmissão do vírus [8].

Até o momento, não existem tratamentos eficazes aprovados contra o ZIKV. O manejo clínico de casos sintomáticos ocorre por meio de medicamentos para amenizar a febre e dor, além de repouso e ingestão de líquidos (MWALIKO et al., 2021). Nos casos de microcefalia, também não há um tratamento específico. Ações de suporte podem auxiliar no desenvolvimento da criança [9]. Adicionalmente, não existem vacinas aprovadas como forma profilática, e apesar da descrição de vacinas promissoras, muitos estudos ainda serão necessários antes que a vacinação esteja disponível para a população [10–12]. Desta forma, novas abordagens terapêuticas necessitam ser desenvolvidas contra a infecção do ZIKV, que incluem a investigação da atividade antiviral de compostos que possam inibir a replicação viral.

Compostos naturais e as toxinas de animais

Os compostos naturais têm um papel importante no desenvolvimento de novos fármacos e, nesse contexto, eles podem servir como alternativas para o desenvolvimento de novas abordagens anti-ZIKV (HARVEY, 2008). Muitos trabalhos reportaram o uso

de compostos extraídos de fontes naturais animais e vegetais como possíveis agentes terapêuticos, inclusive com atividade antiviral contra o ZIKV [13–15].

Dentre os compostos naturais, as peçonhas de serpente têm sido muito utilizadas como modelos terapêuticos, por serem uma mistura complexa de proteínas, como oxidases, lectinas, metalo-proteínas, desintegrinas, enzimas proteolíticas e fosfolipases A2 (PLA2) (PUZARI; FERNANDES; MUKHERJEE, 2022). O isolamento de algumas dessas moléculas permitiu a identificação de um peptídeo da peçonha de *Bothrops jararaca*, responsável pela inibição da Enzima Conversora de Angiotensina (ECA), a qual é amplamente utilizada como agente anti-hipertensivo (Captopril®) (KINI; KOH, 2020).

Dentre estas peçonhas de serpente, os venenos botrópicos representam uma fonte promissora de moléculas valiosas, devido às suas atividades farmacológicas já relatadas, como efeitos antitumorais, antiparasitários, antibacterianos e antivirais (DE MELO ALVES PAIVA et al., 2011; MULLER et al., 2012; CECILIO et al., 2013; BEZERRA et al., 2019; BARBOSA et al., 2021). Sua composição rica em proteínas, resulta em produtos biológicos com atividades potentes e eficientes, que apresentam múltiplos alvos moleculares e funções terapêuticas [16].

Bothropstoxinas I e II de *Bothrops jararacussu*

Bothrops é um gênero de serpentes peçonhentas da família *Viperidae*, encontrado nas Américas Central e do Sul, responsável pelo maior número de acidentes ofídicos nessas regiões (UTKIN, 2015). *Bothrops jararacussu* é conhecida popularmente como jararacuçu, surucucu-dourada ou surucucu-tapete. Esta espécie é encontrada em florestas tropicais, pântanos e margens de rios e, no Brasil, habita desde a Bahia até o Rio Grande do Sul e Mato Grosso do Sul (GRAZZIOTIN et al., 2006). Duas das principais classes de proteínas de venenos botrópicos são as PLA₂s e as metaloproteases, relacionadas principalmente a efeitos miotóxicos (DA SILVA AGUIAR et al., 2020). Quando comparado a outras serpentes mencionadas deste gênero, o veneno de *B. jararacussu* apresenta maior efeito miotóxico, resultando em mioglobínúria e insuficiência renal aguda (MELO et al., 1993).

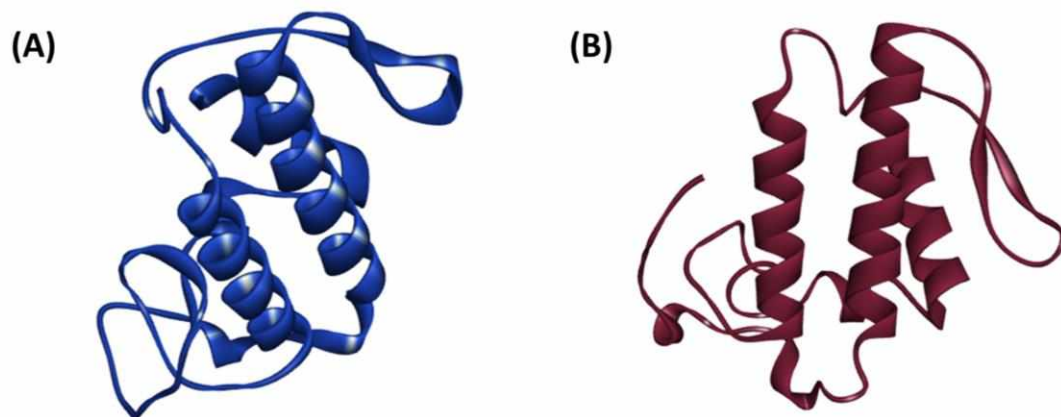
As PLA₂s isoladas do veneno de serpentes têm sido associadas a uma variedade de efeitos terapêuticos (GUTIÉRREZ; LOMONTE, 1995). Elas são conhecidas pela sua atividade como hidrolases, essenciais para o metabolismo de fosfolipídios e para a

regulação de lipídios de membrana, liberando lisofosfolipídios e ácidos graxos livres. (BURKE; DENNIS, 2009). Elas compartilham um mecanismo catalítico conservado, baseado no sítio ativo Histidina/Aspartato (His/Asp), usando cálcio como cofator essencial para a atividade catalítica, e são divididas em dois subgrupos principais, dependendo do resíduo de aminoácido na posição 49 em sua estrutura primária. PLA_{ss} com Aspartato (Asp49) são enzimaticamente ativas, enquanto que PLA_{ss} com Lisina (Lys49) não apresentam atividade enzimática (MARAGANORE et al., 1984; LOMONTE; RANGEL, 2012).

Uma vez que as PLA_{2s} foram descritas anteriormente como possuindo atividades antivirais (FARINHA SHIMIZU et al., 2017; TEIXEIRA et al., 2020; SANTOS et al., 2021), é de grande interesse avaliar o efeito anti-ZIKV de bothropstoxinas (BthTX) isoladas do veneno de *Bothrops jararacussu*, visto que essas PLA_{2s} são dependentes de cálcio, onde estão associadas à membrana e envolvidas no metabolismo dos fosfolipídios (MUKHERJEE; MIELE; PATTABIRAMAN, 1994; TEIXEIRA et al., 2020).

A BthTX-I é uma Lys49 PLA₂ básica, que consiste em uma cadeia de 121 resíduos de aminoácidos, com peso molecular de 13 kDa, apresenta efeitos miotóxicos e não apresenta atividade enzimática (ANDRIÃO-ESCARSO et al., 2000) (**Figura 6A**). Alternativamente, a BthTX-II, uma Asp49 PLA₂ básica, de 122 resíduos de aminoácidos e peso molecular de 13 kDa, também apresenta efeitos miotóxicos, porém, é enzimaticamente ativa e possui uma atividade catalítica (GUTIÉRREZ et al., 1991) (**Figura 6B**), podendo estar envolvida em múltiplas vias de transdução de sinais, possivelmente devido à sua ação enzimática (CORRÊA et al., 2008). BthTX-I demonstrou possuir atividade antiviral contra os vírus Dengue (DENV) e Febre Amarela (YFV), interagindo diretamente com as partículas virais no ensaio virucida, e bloqueando a adsorção e internalização destas (MULLER et al., 2012). Por outro lado, não há relatos na literatura da atividade antiviral de BthTX-II. Portanto, BthTX-I e BthTX-II se apresentam como uma fonte promissora para o desenvolvimento de tratamentos futuros contra a febre Zika.

Figura 6: Estrutura das bothropstoxinas I e II isoladas da peçonha de *Bothrops jararacussu*. BthTX-I (PDB: 3HZD) (A). BthTX-II (PDB: 2OQD) (B).



Adaptado de (CORRÊA et al., 2008; FERNANDES et al., 2010).

OBJETIVOS

O presente trabalho teve como objetivo avaliar a atividade das bothropstoxinas I e II isoladas da peçonha da serpente *Bothrops jararacussu* no ciclo replicativo do ZIKV *in vitro*.

Objetivos específicos

- Determinar a concentração efetiva de 50% (EC_{50}), concentração citotóxica em 50% (CC_{50}) e índice de seletividade ($IS=CC_{50}/EC_{50}$) de BthTX-I e II, de forma a estabelecer os valores ótimos de concentração para o tratamento celular e avaliar o potencial antiviral destas moléculas;
- Avaliar a atividade de BthTX-I e II em diferentes etapas do ciclo replicativo do ZIKV, para um melhor entendimento das etapas do ciclo viral inibidas por essas moléculas.
- Investigar as interações de BthTX-I e II com proteínas do ZIKV por meio de *docking* molecular, para identificar potenciais alvos virais e mecanismos de ação antiviral;
- Analisar por espectroscopia de infravermelho (FTIR) as interações químicas de BthTX-I e II com constituintes da partícula viral do ZIKV, afim de investigar o modo de ação destas moléculas.

REFERÊNCIAS

AGRELLI, A. et al. Zika virus entry mechanisms in human cells. **Infection, Genetics and Evolution**, 2019. <https://doi.org/10.1016/j.meegid.2019.01.018>

ANDRIÃO-ESCARSO, S. H. et al. Myotoxic phospholipases A2 in Bothrops snake venoms: Effect of chemical modifications on the enzymatic and pharmacological properties of bothropstoxins from Bothrops jararacussu. **Biochimie**, v. 82, n. 8, p. 755–763, 2000. [https://doi.org/10.1016/S0300-9084\(00\)01150-0](https://doi.org/10.1016/S0300-9084(00)01150-0)

BARBOSA, L. G. et al. A comparative study on the leishmanicidal activity of the L-amino acid oxidases BjussuLAAO-II and BmooLAAO-II isolated from Brazilian Bothrops snake venoms. **International Journal of Biological Macromolecules**, 2021. <https://doi.org/10.1016/j.ijbiomac.2020.11.146>

BESNARD, M. et al. Evidence of perinatal transmission of zika virus, French Polynesia, December 2013 and February 2014. **Eurosurveillance**, v. 19, n. 13, p. 20751, 2014. <https://doi.org/10.2807/1560-7917.ES2014.19.13.20751>

BERNATCHEZ, J. A. et al. **Drugs for the Treatment of Zika Virus Infection** *Journal of Medicinal Chemistry* American Chemical Society, , 23 jan. 2020.

BEZERRA, P. H. A. et al. BthTX-I from Bothrops jararacussu induces apoptosis in human breast cancer cell lines and decreases cancer stem cell subpopulation. **Journal of Venomous Animals and Toxins Including Tropical Diseases**, v. 25, n. July 2019, p. 1–9, 2019. <https://doi.org/10.1590/1678-9199-jvatitd-2019-0010>

BOIGARD, H. et al. Zika virus-like particle (VLP) based vaccine. **PLoS Neglected Tropical Diseases**, v. 11, n. 5, p. 1–20, 2017. <https://doi.org/10.1371/journal.pntd.0005608>

BOS, S. et al. The structural proteins of epidemic and historical strains of Zika virus differ in their ability to initiate viral infection in human host cells. **Virology**, 2019. <https://doi.org/10.1016/j.virol.2017.12.003>

BRASIL, P. et al. Zika Virus Infection in Pregnant Women in Rio de Janeiro. **New England Journal of Medicine**, v. 375, n. 24, p. 2321–2334, 2016.

BUJALOWSKI, P. J.; BUJALOWSKI, W.; CHOI, K. H. Interactions between the Dengue Virus Polymerase NS5 and Stem-Loop A. **Journal of Virology**, v. 91, n. 11, p.

1–11, 2017. <https://doi.org/10.1128/JVI.00047-17>

BURKE, J. E.; DENNIS, E. A. Phospholipase A2 biochemistry. **Cardiovascular Drugs and Therapy**, v. 23, n. 1, p. 49–59, 18 fev. 2009. <https://doi.org/10.1007/s10557-008-6132-9>

CALVET, G. et al. Detection and sequencing of Zika virus from amniotic fluid of fetuses with microcephaly in Brazil: a case study. **The Lancet Infectious Diseases**, v. 16, n. 6, p. 653–660, 2016. [https://doi.org/10.1016/S1473-3099\(16\)00095-5](https://doi.org/10.1016/S1473-3099(16)00095-5)

CAMPOS, G. S.; BANDEIRA, A. C.; SARDI, S. I. Zika virus outbreak, Bahia, Brazil. **Emerging Infectious Diseases**, v. 21, n. 10, p. 1885–1886, 2015. <https://doi.org/10.3201/eid2110.150847>

CAO-LORMEAU, V. M. et al. Guillain-Barré Syndrome outbreak associated with Zika virus infection in French Polynesia: A case-control study. **The Lancet**, v. 387, n. 10027, p. 1531–1539, 2016. [https://doi.org/10.1016/S0140-6736\(16\)00562-6](https://doi.org/10.1016/S0140-6736(16)00562-6)

CECILIO, A. B. et al. Molecular characterization of Lys49 and Asp49 phospholipases A₂ from snake venom and their antiviral activities against Dengue virus. **Toxins**, v. 5, n. 10, p. 1780–1798, out. 2013. <https://doi.org/10.3390/toxins5101780>

CHRISTIAN, K. M.; SONG, H.; MING, G. L. Pathophysiology and Mechanisms of Zika Virus Infection in the Nervous System. **Annual Review of Neuroscience**, v. 42, p. 249–269, 2019. <https://doi.org/10.1146/annurev-neuro-080317-062231>

CORRÊA, L. C. et al. Crystal structure of a myotoxic Asp49-phospholipase A2 with low catalytic activity: Insights into Ca²⁺-independent catalytic mechanism. **Biochimica et biophysica acta**, v. 1784, n. 4, p. 591–599, abr. 2008. <https://doi.org/10.1016/j.bbapap.2008.01.007>

CORREA DE OLIVEIRA, P. M. et al. Bioprospection for new larvicides against *Aedes aegypti* based on ethnoknowledge from the Amazonian São Sebastião de Marinaú riverside community. **Journal of ethnopharmacology**, v. 293, 15 jul. 2022. <https://doi.org/10.1016/j.jep.2022.115284>

COX, B. D.; STANTON, R. A.; SCHINAZI, R. F. Predicting Zika virus structural biology: Challenges and opportunities for intervention. **Antiviral Chemistry and Chemotherapy**, v. 24, n. 3–4, p. 118–126, 2015. <https://doi.org/10.1177/2040206616653873>

- DA SILVA AGUIAR, W. et al. Ontogenetic study of Bothrops jararacussu venom composition reveals distinct profiles. **Toxicon**, v. 186, p. 67–77, 30 out. 2020. <https://doi.org/10.1016/j.toxicon.2020.07.030>
- DE CASTRO BARBOSA, E. et al. Searching for plant-derived antivirals against dengue virus and Zika virus. **Virology Journal**, v. 19, n. 1, p. 1–15, 2022. <https://doi.org/10.1186/s12985-022-01751-z>
- DE MELO ALVES PAIVA, R. et al. Cell cycle arrest evidence, parasiticidal and bactericidal properties induced by L-amino acid oxidase from Bothrops atrox snake venom. **Biochimie**, 2011. <https://doi.org/10.1016/j.biochi.2011.01.009>
- DICK, G W A et al. “Zika virus. I. Isolations and serological specificity.” **Transactions of the Royal Society of Tropical Medicine and Hygiene** vol. 46,5, p. 509-20, 1952. [https://doi.org/10.1016/0035-9203\(52\)90042-4](https://doi.org/10.1016/0035-9203(52)90042-4)
- DIOSA-TORO, M. et al. Role of RNA-binding proteins during the late stages of Flavivirus replication cycle. **Virology Journal**, v. 17, n. 1, p. 1–14, 2020. <https://doi.org/10.1186/s12985-020-01329-7>
- DUFFY, M. R. et al. Zika Virus Outbreak on Yap Island, Federated States of Micronesia. **New England Journal of Medicine**, v. 360, n. 24, p. 2536–2543, 2009. <https://doi.org/10.1056/NEJMoa0805715>
- FARINHA SHIMIZU, J. et al. Multiple effects of toxins isolated from *Crotalus durissus terrificus* on the hepatitis C virus life cycle. 2017. <https://doi.org/10.1371/journal.pone.0187857>
- FELLNER, C. Zika in America: The year in review. **P and T**, v. 41, n. 12, p. 778–791, 2016.
- FERNANDES, C. A. H. et al. Comparison between apo and complexed structures of bothropstoxin-I reveals the role of Lys122 and Ca(2+)-binding loop region for the catalytically inactive Lys49-PLA(2)s. **Journal of structural biology**, v. 171, n. 1, p. 31–43, jul. 2010. <https://doi.org/10.1016/j.jsb.2010.03.019>
- FOY, B. D. et al. Probable Non-Vector-borne Transmission of Zika Virus, Colorado, USA. **Emerging Infectious Diseases**, v. 17, n. 5, p. 880–882, 2011. <https://doi.org/10.3201/eid1705.101939>
- GAUDINSKI, M. R. et al. Safety, tolerability, and immunogenicity of two Zika virus

DNA vaccine candidates in healthy adults: randomised , open-label, phase 1 clinical trials. **The Lancet**, v. 391, 2018.

GIRALDO, M. I. et al. Envelope protein ubiquitination drives entry and pathogenesis of Zika virus. **Nature**, v. 585, n. 7825, p. 414–419, 2020. <https://doi.org/10.1038/s41586-020-2457-8>

GRAZZIOTIN, F. G. et al. Phylogeography of the Bothrops jararaca complex (Serpentes: Viperidae): past fragmentation and island colonization in the Brazilian Atlantic Forest. **Molecular Ecology**, v. 15, n. 13, p. 3969–3982, 1 nov. 2006. <https://doi.org/10.1111/j.1365-294X.2006.03057.x>

GUTIÉRREZ, J.; LOMONTE, B. Phospholipase A2 myotoxins from Bothrops snake venoms. **Toxicon**, v. 33, n. 11, p. 1405–1424, 1995. [https://doi.org/10.1016/0041-0101\(95\)00085-Z](https://doi.org/10.1016/0041-0101(95)00085-Z)

GUTIÉRREZ, J. M. et al. Skeletal muscle degeneration and regeneration after injection of bothropstoxin-II, a phospholipase A2 isolated from the venom of the snake Bothrops jararacussu. **Experimental and Molecular Pathology**, v. 55, n. 3, p. 217–229, 1991. [https://doi.org/10.1016/0014-4800\(91\)90002-F](https://doi.org/10.1016/0014-4800(91)90002-F)

HACKETT, B. A.; CHERRY, S. Flavivirus internalization is regulated by a size-dependent endocytic pathway. **Proceedings of the National Academy of Sciences of the United States of America**, v. 115, n. 16, p. 4246–4251, 2018. <https://doi.org/10.1073/pnas.1720032115>

HAMEL, R. et al. Biology of Zika Virus Infection in Human Skin Cells. **Journal of virology**, v. 89, n. 17, p. 8880–8896, set. 2015. <https://doi.org/10.1128/JVI.00354-15>

HARVEY, A. Natural products in drug discovery. **Drug Discovery Today**, v. 13, n. 19–20, p. 894–901, out. 2008. <https://doi.org/10.1016/j.drudis.2008.07.004>

HEANG, V. et al. Zika virus infection, Cambodia, 2010. **Emerging Infectious Diseases**, v. 18, n. 2, p. 349–351, 2012. <https://doi.org/10.3201/eid1802.111224>

HENNESSEY, M.; FISCHER, M.; STAPLES, J. E. Zika Virus Spreads to New Areas — Region of the Americas, May 2015–January 2016. **MMWR. Morbidity and Mortality Weekly Report**, v. 65, n. 3, p. 1–4, 2016. <https://doi.org/10.15585/mmwr.mm6503e1er>

JAVED, F. et al. Zika virus: what we need to know? **Journal of Basic Microbiology**

- Wiley-VCH Verlag, , 1 jan. 2018. <https://doi.org/10.1002/jobm.201700398>
- JIMÉNEZ DE OYA, N. et al. Low Immune Cross-Reactivity between West Nile Virus and a Zika Virus Vaccine Based on Modified Vaccinia Virus Ankara. **Pharmaceuticals (Basel, Switzerland)**, v. 15, n. 3, 1 mar. 2022. <https://doi.org/10.3390/ph15030354>
- KIM, J. H. et al. A screening study of high affinity peptide as molecular binder for AXL, tyrosine kinase receptor involving in Zika virus entry. **Bioelectrochemistry**, v. 137, p. 107670, 2021. <https://doi.org/10.1016/j.bioelechem.2020.107670>
- KINI, R. M.; KOH, C. Y. Snake venom three-finger toxins and their potential in drug development targeting cardiovascular diseases. **Biochemical pharmacology**, v. 181, 1 nov. 2020. <https://doi.org/10.1016/j.bcp.2020.114105>
- KWONG, J. C.; DRUCE, J. D.; LEDER, K. Case report: Zika virus infection acquired during brief travel to indonesia. **American Journal of Tropical Medicine and Hygiene**, v. 89, n. 3, p. 516–517, 2013. <https://doi.org/10.4269/ajtmh.13-0029>
- LANCIOTTI, R. S. et al. Genetic and serologic properties of Zika virus associated with an epidemic, Yap State, Micronesia, 2007. **Emerging Infectious Diseases**, v. 14, n. 8, p. 1232–1239, 2008. <https://doi.org/10.3201/eid1408.080287>
- LOMONTE, B.; RANGEL, J. Snake venom Lys49 myotoxins: From phospholipases A2 to non-enzymatic membrane disruptors. **Toxicon**, v. 60, n. 4, p. 520–530, 15 set. 2012. <https://doi.org/10.1016/j.toxicon.2012.02.007>
- MA, X.; YUAN, Z.; YI, Z. Identification and characterization of key residues in Zika virus envelope protein for virus assembly and entry. **Emerging microbes & infections**, v. 11, n. 1, p. 1604–1620, 31 dez. 2022. <https://doi.org/10.1080/22221751.2022.2082888>
- MACNAMARA, F. N. Zika virus: A report on three cases of human infection during an epidemic of jaundice in Nigeria. **Transactions of the Royal Society of Tropical Medicine and Hygiene**, v. 48, n. 2, p. 139–145, 1954. [https://doi.org/10.1016/0035-9203\(54\)90006-1](https://doi.org/10.1016/0035-9203(54)90006-1)
- MAGNUS, M. M. et al. Risk of Zika virus transmission by blood donations in Brazil. **Hematology, Transfusion and Cell Therapy**, v. 40, n. 3, p. 250–254, 2018. <https://doi.org/10.1016/j.htct.2018.01.011>
- MARAGANORE, J. M. et al. A new class of phospholipases A2 with lysine in place of

- aspartate 49. Functional consequences for calcium and substrate binding. **Journal of Biological Chemistry**, v. 259, n. 22, p. 13839–13843, 25 nov. 1984. [https://doi.org/10.1016/S0021-9258\(18\)89822-2](https://doi.org/10.1016/S0021-9258(18)89822-2)
- MARINI, G. et al. First outbreak of Zika virus in the continental United States: A modelling analysis. **Eurosurveillance**, v. 22, n. 37, p. 1–8, 2017. <https://doi.org/10.2807/1560-7917.ES.2017.22.37.30612>
- MASMEJAN, S. et al. Zika Virus. **Pathogens**, v. 9, n. 11, 2020. <https://doi.org/10.3390/pathogens9110898>
- MELO, P. A. et al. Antagonism of the myotoxic effects of Bothrops jararacussu venom and bothropstoxin by polyanions. **Toxicon**, v. 31, n. 3, p. 285–291, 1 mar. 1993. [https://doi.org/10.1016/0041-0101\(93\)90146-A](https://doi.org/10.1016/0041-0101(93)90146-A)
- MLAKAR, J. et al. Zika Virus Associated with Microcephaly. **New England Journal of Medicine**, v. 374, n. 10, p. 951–958, 2016. <https://doi.org/10.1056/NEJMoa1600651>
- MOHD ROPIDI, M. I. et al. Endoplasmic reticulum: A focal point of Zika virus infection. **Journal of Biomedical Science**, v. 27, n. 1, p. 1–13, 2020. <https://doi.org/10.1186/s12929-020-0618-6>
- MS, M. DA S. Monitoramento dos casos de arboviroses até a semana epidemiológica 9 de 2022. [s.l: s.n.]. v. 53
- MUKHERJEE, A. B.; MIELE, L.; PATTABIRAMAN, N. Phospholipase A2 enzymes: Regulation and physiological role. **Biochemical Pharmacology**, v. 48, n. 1, p. 1–10, 1994. [https://doi.org/10.1016/0006-2952\(94\)90216-X](https://doi.org/10.1016/0006-2952(94)90216-X)
- MULLER, V. D. M. et al. Crotoxin and phospholipases A 2 from Crotalus durissus terrificus showed antiviral activity against dengue and yellow fever viruses. **Toxicon**, v. 59, n. 4, p. 507–515, 2012. <https://doi.org/10.1016/j.toxicon.2011.05.021>
- MWALIKO, C. et al. Zika virus pathogenesis and current therapeutic advances. **Pathogens and Global Health**, v. 115, n. 1, p. 21–39, 2021. <https://doi.org/10.1080/20477724.2020.1845005>
- OEHLER, E. et al. Zika virus infection complicated by guillain-barré syndrome "case report, French Polynesia, December 2013. **Eurosurveillance**, v. 19, n. 9, p. 7–9, 2014. <https://doi.org/10.2807/1560-7917.ES2014.19.9.20720>

- ORTONI, G. E. et al. Factors related to the quality of life of mothers of children with Congenital Zika Virus Syndrome. **Revista gaucha de enfermagem**, v. 43, 2022. <https://doi.org/10.1590/1983-1447.2022.20200374.en>
- PIELNAA, P. et al. Zika virus-spread, epidemiology, genome, transmission cycle, clinical manifestation, associated challenges, vaccine and antiviral drug development. **Virology**, v. 543, n. October 2019, p. 34–42, 2020. <https://doi.org/10.1016/j.virol.2020.01.015>
- PIERSON, T. C.; DIAMOND, M. S. The continued threat of emerging flaviviruses. **Nature Microbiology**, v. 5, n. 6, p. 796–812, 2020. <https://doi.org/10.1038/s41564-020-0714-0>
- PUZARI, U.; FERNANDES, P. A.; MUKHERJEE, A. K. Pharmacological re-assessment of traditional medicinal plants-derived inhibitors as antidotes against snakebite envenoming: A critical review. **Journal of ethnopharmacology**, v. 292, p. 115208, jun. 2022. <https://doi.org/10.1016/j.jep.2022.115208>
- RAMAN et al. Vector control operations framework for Zika virus. **World Health Organization**, p. 4–10, 2016.
- RICHNER, J. M. et al. Modified mRNA Vaccines Protect against Zika Virus Article Modified mRNA Vaccines Protect against Zika Virus Infection. **Cell**, v. 168, n. 6, p. 1114- 1125.e10, 2017. <https://doi.org/10.1016/j.cell.2017.02.017>
- ROIZ, D. et al. Integrated Aedes management for the control of Aedes-borne diseases. **PLoS Neglected Tropical Diseases**, v. 12, n. 12, p. 1–21, 2018. <https://doi.org/10.1371/journal.pntd.0006845>
- RONG, H. et al. Self-Assembling Nanovaccine Confers Complete Protection Against Zika Virus Without Causing Antibody-Dependent Enhancement. **Frontiers in immunology**, v. 13, 9 maio 2022. <https://doi.org/10.3389/fimmu.2022.905431>
- ROZÉ, B. et al. Zika virus detection in urine from patients with Guillain-Barré syndrome on Martinique, January 2016. **Eurosurveillance**, v. 21, n. 9, p. 8–11, 2016. <https://doi.org/10.2807/1560-7917.ES.2016.21.9.30154>
- SANTOS, I. A. et al. Chikungunya virus entry is strongly inhibited by phospholipase A2 isolated from the venom of *Crotalus durissus terrificus*. **Scientific Reports**, v. 11, n. 1, p. 1–12, 2021. <https://doi.org/10.1038/s41598-021-88039-4>

SARNO, M. et al. Zika Virus Infection and Stillbirths: A Case of Hydrops Fetalis, Hydranencephaly and Fetal Demise. **PLoS Neglected Tropical Diseases**, v. 10, n. 2, p. 5–9, 2016. <https://doi.org/10.1371/journal.pntd.0004517>

SCHULER-FACCINI, L. et al. Possible Association Between Zika Virus Infection and Microcephaly — Brazil, 2015. **MMWR. Morbidity and Mortality Weekly Report**, v. 65, n. 3, p. 59–62, 2016. <https://doi.org/10.15585/mmwr.mm6503e2>

SHAN, C. et al. A live-attenuated Zika virus vaccine candidate induces sterilizing immunity in mouse models. **Nature Publishing Group**, v. 23, n. 6, p. 763–767, 2017. <https://doi.org/10.1038/nm.4322>

SHARMA, V. et al. Zika virus: An emerging challenge to public health worldwide. **Canadian Journal of Microbiology** Canadian Science Publishing, , 2020. Disponível em: <<https://pubmed.ncbi.nlm.nih.gov/31682478/>>. Acesso em: 18 fev. 2021

STRANGE, D. P. et al. Axl Promotes Zika Virus Entry and Modulates the Antiviral State of Human Sertoli Cells. **American Society for Microbiology**, v. 10, n. 4, p. 1–16, 2019. <https://doi.org/10.1128/mBio.01372-19>

SUMMERS, D. J.; ACOSTA, R. W.; ACOSTA, A. M. Zika Virus in an American Recreational Traveler. **Journal of Travel Medicine**, v. 22, n. 5, p. 338–340, 2015. <https://doi.org/10.1111/jtm.12208>

TAN, T. Y. et al. Capsid protein structure in Zika virus reveals the flavivirus assembly process. **Nature Communications**, v. 11, n. 1, p. 1–13, 2020. <https://doi.org/10.1038/s41467-020-14647-9>

TAPPE, D. et al. First case of laboratory-confirmed zika virus infection imported into Europe, November 2013. **Eurosurveillance**, v. 19, n. 4, p. 1–4, 2014. <https://doi.org/10.2807/1560-7917.ES2014.19.4.20685>

TAPPE, D. et al. Acute Zika virus infection after travel to Malaysian Borneo, September 2014. **Emerging Infectious Diseases**, v. 21, n. 5, p. 911–913, 2015. <https://doi.org/10.3201/eid2105.141960>

TEIXEIRA, S. C. et al. Insights into the antiviral activity of phospholipases A 2 (PLA 2 s) from snake venoms. n. January, 2020. <https://doi.org/10.1016/j.ijbiomac.2020.07.178>

UTKIN, Y. N. Animal venom studies: Current benefits and future developments.

World Journal of Biological Chemistry, v. 6, n. 2, p. 28, 2015.
<https://doi.org/10.4331/wjbc.v6.i2.28>

VICTORA, C. G. et al. Microcephaly in Brazil: How to interpret reported numbers? **The Lancet**, v. 387, n. 10019, p. 621–624, 2016. [https://doi.org/10.1016/S0140-6736\(16\)00273-7](https://doi.org/10.1016/S0140-6736(16)00273-7)

VOLPI, V. G. et al. Zika Virus Replication in Dorsal Root Ganglia Explants from Interferon Receptor1 Knockout Mice Causes Myelin Degeneration. **Scientific reports**, v. 8, n. 1, 1 dez. 2018. <https://doi.org/10.1038/s41598-018-28257-5>

WHO. **WHO guidelines for the prevention of sexual transmission of Zika virus**. 2020.

WHO, W. H. O. Zika virus outbreaks in the Americas. **Weekly epidemiological record / Health Section of the Secretariat of the League of Nations**, v. 90, n. 45, p. 609–610, 2015.

WHO, W. H. O. Zika virus, microcephaly and Guillain-Barre syndrome. Situation report 05-January-2017. p. 1–13, 2016.

WHO, W. H. O. Zika Epidemiology Update. **Who**, n. July, p. 1–14, 2019.

ZANLUCA, C. et al. First report of autochthonous transmission of Zika virus in Brazil. **Memorias do Instituto Oswaldo Cruz**, v. 110, n. 4, p. 569–572, 2015.
<https://doi.org/10.1590/0074-02760150192>

CAPÍTULO II

Manuscript:

**ROLES OF *BOTHROPS JARARACUSSU* TOXINS I AND II:
ANTIVIRAL FINDINGS AGAINST ZIKA VIRUS**

*Este capítulo está em formato de manuscrito com algumas alterações estruturais para melhor se adequar ao formato da dissertação. O artigo em questão será submetido à revista **International Journal of Biological Macromolecules**.

ROLES OF *BOTHROPS JARARACUSSU* TOXINS I AND II: ANTIVIRAL FINDINGS AGAINST ZIKA VIRUS

Natasha Marques Cassani¹, Igor Andrade Santos¹, Victória Riquena Grosche^{1,2}, Giulia Magalhães Ferreira¹, Marco Guevara-Vega¹, Rafael Borges Rosa^{3,4}, Lindomar José Pena⁴, Nilson Nicolau-Junior⁵, Adélia Cristina Oliveira Cintra⁶, Robinson Sabino-Silva¹, Suely Vilela Sampaio⁶, Ana Carolina Gomes Jardim^{1,2}.

¹Institute of Biomedical Science (ICBIM), Federal University of Uberlândia (UFU), Uberlândia, Minas Gerais, Brazil.

²Institute of Biosciences, Humanities and Exact Sciences (Ibilce), São Paulo State University (Unesp), São José do Rio Preto, SP, Brazil.

³Rodents Animal Facilities Complex, Federal University of Uberlândia, Uberlândia, Minas Gerais, Brazil.

⁴Department of Virology, Aggeu Magalhães Institute (IAM), Oswaldo Cruz Foundation (Fiocruz), Recife, Brazil.

⁵Institute of Biotechnology, Federal University of Uberlândia (UFU), Uberlândia, Minas Gerais, Brazil.

⁶Department of Clinical Analyses, Toxicology and Food Sciences, School of Pharmaceutical Sciences of Ribeirão Preto, University of São Paulo – USP, Ribeirão Preto, SP, Brazil.

Corresponding author: Professor Ana Carolina Gomes Jardim, Institute of Biomedical Science (ICBIM), Federal University of Uberlandia (UFU), Avenida Amazonas, 4C-Room 216, Umuarama, Uberlândia, Minas Gerais, Brazil, CEP: 38405-302.

Tel: +55 (34) 3225-8682

E-mail: jardim@ufu.br

Keywords: antiviral drugs; zika virus; toxins.

ABSTRACT

Zika virus is the etiologic agent of Zika fever, and has been previously associated with cases of microcephaly, drawing the attention of the health authorities worldwide. However, no vaccine or antiviral are currently available. Phospholipases A₂ (PLA₂) isolated from snake venoms have demonstrated antiviral activity against several viruses. Here we demonstrated the anti-ZIKV activity of bothropstoxins-I and II (BthTX-I and II) isolated from *Bothrops jararacussu* venom. Vero E6 cells were infected with ZIKV_{PE243} in the presence of compounds for 72 hours, when virus titers were evaluated. BthTX-I and II presented strong dose-dependent inhibition of ZIKV, with a SI of 149.1 and 1.44×10^5 , respectively. These toxins mainly inhibited the early stages of the replicative cycle, such as during the entry of ZIKV into host cells, as shown by the potent virucidal effect, suggesting the action of these toxins on the virus particles. Moreover, BthTX-I and II presented significant activity towards post-entry stages of the ZIKV replicative cycle. Molecular docking analyses showed that BthTX-I and II potentially interact with DII and DIII domains from ZIKV Envelope protein. Our findings show that these PLA₂s could be used as useful templates for the development of future antiviral candidate drugs against Zika fever.

1. INTRODUCTION

Zika fever is a disease caused by Zika virus (ZIKV), an arthropod-transmitted virus which belongs to the *Flaviviridae* family [1]. ZIKV particles are characterized by an approximate size of 40-60 nm in diameter, with an icosahedral capsid, and a lipid envelope into which the Envelope (E) and matrix protein (E) are inserted[2]. The E protein is the major structural protein related to the interaction with host receptors and immune recognition[3]. Its genome consists of a positive sense single stranded RNA of 11 kb, with a single open reading frame (ORF), which encodes a polyprotein that is cleaved into three structural proteins [E, capsid (C) and membrane (M) proteins], and seven non-structural proteins (NS1, NS2A, NS2B, NS3, NS4A, NS4B and NS5) [4].

ZIKV transmission occurs through the bite of mosquitoes from the genus *Aedes*, being the major species the *Aedes aegypti* and *Aedes albopictus* [5]. However, unlike other arboviruses, it can also be transmitted by sexual contact [6], vertically[7], and blood transfusion [8]. Transmission through the placenta can result in congenital Zika syndrome, characterized by microcephaly and other teratogenies [9], which represented

a considerable health problem that Brazil faced in 2016, resulting in long-term consequences [10]. Therefore, cases of abortion in ZIKV-infected pregnant women, high rates of newborns with microcephaly, and the increase in number of cases of Guillain-Barre syndrome in adults, related to the presence of the virus in Brazil [11], have demonstrate the need to develop an effective antiviral therapy. Currently, the treatment of Zika fever and ZIKV-related diseases are only palliative, to alleviate the symptoms of infected patients [12].

Natural compounds have an important role in the development of new drugs. Among products isolated from animals, bothropic venoms represent a promising source of valuable molecules, due to their previously reported pharmacological activities, such as antitumor, antiparasitic, antibacterial and antiviral effects [13–19]. They are characterized by a complex mixture of proteins resulting in strong and efficient biological products that present multiple molecular targets and functions [20].

Phospholipases A₂ (PLA₂s) are some of the isolated proteins from the venom of snakes, which have been associated with a variety of therapeutic effects [21]. Since PLA₂s have been previously described to possess antiviral activities [22–24], it is of a great interest to evaluate the antiviral effect of bothropstoxins (BthTX) isolated from the venom of *Bothrops jararacussu*, a highly venomous snake endemic to South America.. These PLA₂s are calcium-dependent, which are membrane associated and involved in phospholipid metabolism [22,25].

BthTX-I (**Figure 1A**), is a basic Lys49 PLA₂, which shows myotoxic effects and presents no enzymatic activity [26]. In the same way, BthTX-II (**Figure 1B**), a second basic Asp49 PLA₂, also presents myotoxic effects, however, is enzymatically active, with a catalytic activity [26]. It is involved in multiple signal transduction pathways, possibly due to its enzymatic action [27]. Nonetheless, the effectiveness of these proteins against ZIKV infection has not been elucidated yet.

Here we evaluated the antiviral activity of BthTX-I and BthTX-II from *Bothrops jararacussu* venom on ZIKV infection through *in vitro* and *in silico* analyses.

2. METHODS

2.1. Phospholipases A₂

The crude venom of *Bothrops jararacussu* was obtained from the “Animal Toxin Extraction Center” (CETA), duly registered and approved by the Ministry of the

Environment under de process number 3002678. The venom was collected from 28 specimens from the Morungaba-SP collection under the Brazilian Institute for the Environment and Renewing Natural Resources (IBAMA) authorization (1/35/1998/000846–1), and extraction was performed by Jairo Marques do Vale (CETA). All experiments were performed in accordance with all relevant guidelines and regulations of the Brazilian federal universities, IBAMA and the Ministry of Environment. The isolation and purification of phospholipases BthTX-I (**Figures 1A**) and BthTX-II (**Figure 1B**) from the venom of *Bothrops jararacussu* snake were carried out at the School of Pharmaceutical Sciences of Ribeirão Preto, University of São Paulo, as previously described [28,29]. The lyophilized protein was dissolved in Phosphate buffer saline (PBS), filtered, and stored at -80°C. Concentrations of each protein after dissolution were confirmed by quantification in colorimetric assay using the kit Pierce BCA Protein Assay (ThermoFisher). Dilutions of the stock solution containing the protein were made immediately prior to the experiments. For all the performed assays, PBS was used as the untreated control. All authors complied with the ARRIVE guidelines.

2.2. Cell culture

Vero E6 cells (kidney tissue derived from a normal adult African green monkey, ATCC E6) were cultured in Dulbecco's modified Eagle's medium (DMEM; Sigma–Aldrich) supplemented with 100 U/mL penicillin (Gibco Life Technologies), 100 mg/mL streptomycin (Gibco Life Technologies), 1% (v/v) non-essential amino acids (Gibco Life Technologies) and 10% (v/v) fetal bovine serum (FBS; Hyclone) at 37 °C in a humidified 5% CO₂ incubator [30].

2.3. Cell viability assay

Cell viability was measured by MTT [3-(4, 5-dimethylthiazol-2-yl)-2, 5-diphenyl tetrazolium bromide] (Sigma–Aldrich) method. Vero E6 cells were seeded in 96-well plates at a density of 5×10^3 cells per well and incubated overnight at 37 °C in a humidified 5% CO₂ incubator as previously described [30], with modifications. Drug-containing medium at concentrations ranging from 0.122 to 250 µg/mL in two-fold serial dilution for BthTX-I and 0.005 ng/mL to 250 µg/mL in five-fold serial dilution for BthTX-II was added to the cell culture for 72 h at 37 °C. Then, the media was

removed and a solution containing MTT at the final concentration of 1 mg/mL was added to each well, incubated for 30 min at 37 °C in a humidified 5% CO₂ incubator, after which media was replaced with 100 µL of DMSO (dimethyl sulfoxide) to solubilize the formazan crystals. Absorbance was measured by optical density (OD) of each well at 490 nm, using the Glomax microplate reader (PROMEGA). Cell viability was calculated according to the equation $(T/C) \times 100\%$, where T and C represent the mean optical density of the treated group and vehicle control group, respectively. The cytotoxic concentration of 50% (CC₅₀) was calculated using Graph Pad Prism 8.0 [30].

2.4. Virus assays

A wild type ZIKV isolate from a clinical sample of a patient in Brazil (ZIKV_{PE243}) [31] was amplified in Vero E6 cells seeded in 75 cm² flask for 3 days. Then, the viral supernatant was collected and stored at -80 °C. To determine viral titers, 5 x 10³ Vero E6 cells were seeded in each of 96 wells plate 24 hours prior to the infection. Cells were infected with 10-fold serially dilution of ZIKV_{PE243} and incubated for 72h in a humidified 5% CO₂ incubator at 37°C. Then, cells were fixed with 4% formaldehyde, washed with PBS and added of blocking buffer (BB) containing 0.1% Triton X-100 (Vetec Labs, BR), 0.2% bovine albumin (BSA) and PBS for 30 min, to perform immunofluorescence assay. Cells were incubated with primary rabbit polyclonal anti-NS3 antibody diluted in BB for 1h. Alexa Fluor 488 conjugated anti-rabbit IgG was used as secondary antibody (Abcam, Cambridge, UK), incubated for 1h. Images were analyzed at EVOs Cell Imaging Systems Fluorescence Microscopy (Thermo Fisher Scientific) and focus of infection were counted and measured as Focus Forming Unit (FFU).

To determine the effective concentration of 50% (EC₅₀) of each toxin, Vero cells were seeded at density of 5 × 10³ cells per well into 96-well plates 24 h prior to the infection. ZIKV_{PE243} at a multiplicity of infection (MOI) of 0.01 and compound at concentrations ranging from 0.122 to 250 µg/mL for BthTX-I and 0.005 ng/mL to 250 µg/mL for BthTX-II were simultaneously added to cells. 72 hours post-infection (h.p.i.), cells were fixed with paraformaldehyde 4%, washed with PBS and immunofluorescence assay was performed. FFU under treatment with each toxin or untreated control were counted. The antiviral activity was calculated according to the equation $(T/C) \times 100\%$, where T and C represent the mean of the treated group and vehicle control, respectively. The effective

concentration of 50% inhibition (EC_{50}) was calculated using Prism 8.0 (Graph Pad). The values of CC_{50} and EC_{50} were used to calculate the selectivity index ($SI = CC_{50}/EC_{50}$).

2.5. Time-of-addition assays

Vero E6 cells at the density of 5×10^3 cells per well were seeded in 96 well plates 24h prior infection and treatment. All infections were performed at MOI of 0.01, efficiency of virus replication was assessed by measurement of FFU 72 h.p.i., and PBS was used as untreated control. In pretreatment assay, cells were treated for 2h with BthTX-I or BthTX-II prior to the ZIKV infection, washed with PBS and added of ZIKV_{PE243} for 2h. Then, cells were washed with PBS and added of fresh medium for 72h. In entry inhibition assay, cells were infected using media-containing compound and virus for 2h, washed with PBS and incubated with fresh medium for 72h. The virucidal activity was assessed using the same protocol of entry assay, except that inoculum containing compound and virus was incubated for 2h before it was added to the cells. In post-entry assay, cells were infected with ZIKV for 2h, washed extensively with PBS to remove unbound virus, and then incubated with medium containing compound for 72h.

2.6. Molecular docking analysis

A protein-protein blind docking analysis was performed, without defining a specific binding site, between the E protein of the ZIKV (PDB: 5HJM) and BthTX-I (PDB: 3HZD) or BthTX-II (PDB: 2OQD). For this purpose, the HDOCK server [32] was used to perform the docking analysis based on a hybrid algorithm based on a template and ab initio modeling. From the anchoring result, 3D images of the complexes were generated using Chimera [33], as well as 2D analysis of the interactions using LigPlot+ [34].

2.7. Infrared spectroscopy: spectral data analysis

The samples were recorded in attenuated total reflection (ATR)-Fourier transform infrared (FTIR) spectroscopy (Agilent Cary 630 FTIR, Agilent Technologies, Santa Clara, CA, USA). The diamond unit in the ATR system performs an internal-reflection element to record the fingerprint infrared signature at 1800 cm^{-1} to 800 cm^{-1} regions.

The samples were prepared using BthTX-I and BthTX-II at 12 µg/mL and ZIKV at a MOI of 0.01. A volume of 1 µL of each sample was inserted on the diamond cell and dehydrated for 5 min using airflow, being this procedure repeated a minimum of 5 times until each sample forms a thin layer on the ATR-crystal. The spectra were then recorded (2 cm⁻¹ resolution, 64 scans). The second derivative spectra were created based on original data plotted in the Origin Pro 9.0 (OriginLab, Northampton, MA, USA) software and adjusted using Savitzky-Golay algorithm with polynomial order 2 and 20 points of the window [30].

2.8. Statistical analysis

Individual experiments were performed in quadruplicates and all assays were performed a minimum of three times to confirm the reproducibility of the results. GraphPad Prism 8.0 software was used to assess statistical differences of means of readings using Student's unpaired t-test or Mann-Whitney tests. P values <0.0001 (****) were considered statistically significant.

3. RESULTS

3.1. BthTX-I and II exhibit strong anti-ZIKV activity *in vitro*

We assessed the anti-ZIKV activity of BthTX-I (**Figure 1A**) and II (**Figure 1B**) using Vero E6 cells and ZIKV_{PE243}. The antiviral activity was evaluated by performing a dose-response assay to determine the effective concentration of 50% (EC₅₀) and cytotoxicity of 50% (CC₅₀). Vero E6 cells were infected with ZIKV_{PE243} and simultaneously treated with BthTX-I at concentrations ranging from 0.122 to 250 µg/mL in two-fold serial dilutions (**Figure 1C**), and with BthTX-II at concentrations ranging from 0.005 ng to 250 µg/mL in five-fold serial dilutions (**Figure 1D**). FFU were assessed 72 h.p.i. In parallel, cell viability was performed by MTT assay. Both PLA₂s were found to be able to inhibit up to 100% of ZIKV replication, while the cell viability under the treatment with toxins at the highest concentration was over 26% for BthTX-I and 52% for BthTX-II. From these range of concentrations, it was determined that BthTX-I has the EC₅₀ of 1.281 µg/mL, CC₅₀ of 191.4 µg/mL, and the Selectivity Index (SI) of 149.4 (**Figure 1C**), while BthTX-II has the EC₅₀ of 1.134 ng/mL, CC₅₀ of

163.6 $\mu\text{g}/\text{mL}$ and the SI of 1.44×10^5 (**Figure 1D**). Therefore, both BthTX-I and II exhibit a potent anti-ZIKV activity, with BthTX-II having the highest SI value.

3.2. BthTX-I and BthTX-II inhibit entry of ZIKV into the host cells

Time-of-addition experiments were performed to analyze the effect of BthTX-I and II on different stages of the ZIKV replication cycle. For all of these assays, infections were performed at MOI of 0.01 for 72 h, and cells were treated with PLA₂s at 12 $\mu\text{g}/\text{mL}$, a concentration that inhibited virus replication by 100% with no significant effect on cell viability in the dose-response assay (**Figures 1C and 1D**).

To assess the PLA₂s effect on ZIKV entry to the host cells, virus and toxins were simultaneously added to Vero E6 cells for 2h at 37 °C, cells were extensively washed with PBS and replaced with fresh medium. FFU were counted 72 h.p.i (**Figure 2A**). BthTX-I and II demonstrated to block 99.4% and 100% of ZIKV replication ($p < 0.0001$), respectively, compared to PBS control, indicating that these compounds are capable to inhibit the ZIKV_{PE243} entry to the host cells (**Figure 2A**). Additionally, the incubation of the inoculum containing BthTX-I or BthTX-II and ZIKV at 37 °C for 2h prior to the infection/treatment of cells strongly inhibited virus replication by 100% ($p < 0.0001$) (**Figure 2B**), demonstrating that PLA₂s also have virucidal activity. Taken together, these data indicate that BthTX-I and BthTX-II possess a potent virucidal activity and a great capacity to block virus entry into host cells.

3.3. BthTX-II protects cells against ZIKV infection

To evaluate the protective effects of PLA₂s against ZIKV infection, cells were pretreated with BthTX-I and II for 2h at 37 °C, washed extensively with PBS to remove the compounds, and infected with ZIKV_{PE243} for 2h. Then, the supernatant was removed, cells were washed, added of fresh medium, and FFU were counted 72 h.p.i (**Figure 3A**). The results demonstrated that BthTX-II, but not BthTX-I, significantly reduced ZIKV_{PE243} infection by 100% ($p < 0.0001$) (**Figure 3A**), demonstrating a robust protective effect against ZIKV infection.

3.4. BthTX-I and BthTX-II interfere with the post-entry stages of ZIKV replication cycle

Finally, to investigate whether BthTX-I and II could interfere with the post-entry stage of ZIKV infection, Vero E6 cells were incubated with ZIKV_{PE243} for 2h, and then the supernatant was removed, cells were extensively washed with PBS to remove unbound virus and added of medium containing BthTX-I or BthTX-II. FFU were measured 72 h.p.i. (**Figure 3B**). Data showed that BthTX-I and BthTX-II decreased up to 57% and 95% of viral replication ($p < 0.0001$), respectively (**Figure 3B**).

From the analysis of the effect of BthTX-I and BthTX-II on the different stages of ZIKV replicative cycle, the results demonstrated that: 1) these compounds mainly affect early stages of infections, inhibiting virus entry to the host cells (**Figure 2**), probably due to an effect of virus particles; 2) BthTX-II protects cells against ZIKV infection and interferes with the post-entry stages (**Figure 3**), the latest may be a residual effect of the treatment of cells prior to the infection; and 3) BthTX-I, differently of BthTX-II, showed a modest yet significant post-entry effect and did not protected cells against infection (**Figure 3**), suggesting that the post-entry activity observed for BthTX-II may be related to an interference on virus replication, affecting the late stages of ZIKV infection, possibly due to its catalytic activity.

3.5 *In silico* analyses suggest interactions of BthTX-I and BthTX-II with ZIKV envelope protein E

Molecular docking calculations were performed to investigate virus-toxins interactions and reveal a potential binding mode between BthTX-I or II and ZIKV envelope protein (E) (**Figure 4**). After docking, the solutions with the highest score for each protein were selected. The docking of both PLA₂s with E protein was predicted between domains II and III (DII and DIII) (**Figure 4**). BthTX-I was predicted to interact with E with global energy of -240.65 kJ/mol, while BthTX-II was also predicted to interact with E, but with an energy of -244.08 kJ/mol, after refining.

The 2D interactions between the PLA₂s and ZIKV E protein showed that the chain C of BthTX-I mainly interacts with chains A and B of E protein, forming eight hydrophobic interactions in A (residues Phe3, Lys70, Leu2 in BthTX-I and Leu96, Gly78, Ser112, Lys110, Thr76 in E protein) and eighteen hydrophobic interactions in B (residues Lys129, Gly33, Lys53, Val31, Cys126, Leu32, Lys122, Leu121, His120, Pro68 in BthTX-I and Ser403, His399, Trp400, His398, Phe314, Ser405, Pro318, Ile317 in E protein) (**Figure 5A**). Furthermore, BthTX-I forms one hydrogen bond with E, Arg72

and Glu79 (2.82 Å) in chain A and one hydrogen bond, His401 and Arg34 in chain B. There is also a salt bridge with E, Asp384 and Arg34 (**Figure 5A**).

Moreover, the chain C of BthTX-II interacts with ZIKV E protein in the same chains: in chain A, forming twenty-two hydrophobic interactions (residues Gly80, Tyr75, Thr13, Tyr21, Lys115, Leu17, Lys11, Gly14, Lys16, Leu110, Leu10, Gln7 in BthTX-II and Ile396, His398, His401, Ser405, Pro318, Thr406, Ile317, Ser403, Glu320, Ala319 in E protein), and in chain B, forming thirteen hydrophobic interactions (residues Trp3, Leu2, Phe19, Pro18, Leu10, Gly6, Leu17 in BthTX-II and Gly106, Gln77, Lys110, Thr76, Leu107, Phe108 in E protein) (**Figure 5B**). Two hydrogen bonds are formed in Arg77 and His399 (2.93 Å and 2.65 Å, respectively) and Glu78 and Asn79 with Thr397 (3.03 Å and 3.21 Å, respectively) (**Figure 5B**).

3.6. BthTX-I and II causes molecular changes in ZIKV particle.

To further investigate the interactions between BthTX-I and II with ZIKV particles, infrared spectral analysis of ZIKV and/or PLA₂s was performed in ATR-FTIR. The representative mean infrared spectra of ZIKV prior and after the incubation with BthTX-I and BthTX-II are showed in **Figures 6A** and **Figure 6B**, respectively. The bio-fingerprint in the range of 1800–800 cm⁻¹ indicates absorption bands of glycoproteins, proteins, lipids, and RNA of virus and may be exploited to suggest the interaction between ZIKV constituents and BthTX-I or II. The second derivative spectrum is capable to identify the accurate spatial distribution of each wavenumber referring to each biochemical component present in the sample [35,36]. In this context, infrared spectra can also detect binding between different functional groups of materials and biological samples [37]. We highlighted the functional groups when a novel vibrational mode characterized by valley in the second derivative spectra was earned with the incubation with ZIKV + BthTX-I or ZIKV + BthTX-II, and when a vibrational mode present in ZIKV was absent after incubation with ZIKV + BthTX-I or ZIKV + BthTX-II. Regarding to the BthTX-I, the vibrational mode at 1717 cm⁻¹ (**Figure 6C**) was detected only after incubation of ZIKV + BthTX-I, suggesting formation of C=O stretching vibration in Amide I of proteins by the interaction of ZIKV + BthTX-I [38]. On the other hand, the vibrational modes at 1317 cm⁻¹ (**Figure 6E**) and 953 cm⁻¹ (**Figure 6G**) were clearly detected in ZIKV, and these respective vibrational modes were absent in ZIKV + BthTX-I, which can suggest interactions of viral particles with

BthTX-I. The vibrational modes at 1317 cm^{-1} and 953 cm^{-1} were respectively related to amide III in proteins [39] and sugar moieties of glycosylated proteins [40], suggesting interaction of viral surface proteins with BthTX-I.

Regarding to the BthTX-II, the vibrational modes at 1705 cm^{-1} (**Figure 6D**), 1527 cm^{-1} (**Figure 6F**), and 1317 cm^{-1} (**Figure 6H**) were clearly detected in ZIKV and these respective vibrational modes were absent in ZIKV + BthTX-II, which can suggest several interactions of viral particles with this toxin. The vibrational modes at 1705 cm^{-1} and 1527 cm^{-1} were, respectively, related to C=O vibrations of guanine and C=N guanine [39]. Guanine is a nucleobase found in the RNA, suggesting an effect of BthTX-II in genomic RNA of ZIKV. In a similar coupled mechanism described to BthTX-I, the vibrational modes at 1317 cm^{-1} was also described only in the ZIKV samples, which can be related with amide III [39] in surface proteins. Otherwise, the vibrational modes at 1327 cm^{-1} (**Figure 6H**) was detected only after incubation of ZIKV + BthTX-II, suggesting formation of alpha-helix bands for Amide III proteins [41].

4. Discussion

PLA₂s are a well-known class of enzymes, widely distributed in nature, essential for the regulation of membrane lipids, since they catalyze the glycerophospholipids, releasing free fatty acid and lysophospholipids [42,43]. Multiple studies have demonstrated the antiviral activity of PLA₂s against several viruses [22–24,44]. In this scenario, these proteins have emerged as potential therapeutic templates to the development of drugs [20]. Here we show the antiviral activity of bothropstoxins-I and II (BthTX-I and II) isolated from the venom of *Bothrops jararacussu* on ZIKV replicative cycle. BthTX-I and II showed a very potent dose-dependent inhibition of ZIKV *in vitro*, with high SI values. The inhibition of viral infection was mainly in the early stages of the replicative cycle, interfering with virus entry into host cells, possible by an effect on virus particles, demonstrated by their strong virucidal effect. Our data are in accordance with previous studies, which showed that PLA₂s from *Crotalus durissus terrificus* inhibited the early stages of the replication cycle of flavivirus, such as Dengue (DENV), Yellow Fever (YFV) and Hepatitis C virus (HCV) [16,24], and alphavirus, such as Chikungunya virus (CHIKV) [23].

Apart from the potent anti-ZIKV activity of both bothropstoxins, our data demonstrated that BthTX-II presented SI 1000 folds higher than BthTX-I, which may be explained by the enzymatic activity of BthTX-II, a catalytic PLA₂ [26]. These results suggest that the catalytic activity may be an important factor for the antiviral effect of PLA₂s, corroborating with the findings of Mitsuishi and colleagues, who demonstrated the catalytic activity of PLA₂s against adenovirus infection [45]. Additionally, only BthTX-II was able to protect cells against ZIKV infection, possibly due to its enzymatic activity on the cell membrane. These results are in agreement with Siniavin and coworkers, which revealed the protective effect of different types of PLA₂s against SARS-CoV-2 infection [46]. Furthermore, when cells were treated with BthTX-II after viral entry, this protein also significantly inhibit post-entry stages of ZIKV replication, suggesting that this may be a residual effect of the protective action, or be due to the catalytic effect of this toxin on the membranes associated to the ZIKV replication complex [24]. Alternatively, BthTX-I showed a modest yet significant post-entry effect and did not protected cells against infection, emphasizing that the activity observed for BthTX-II on the later stages of the infection may be related to its catalytic activity. The post-entry effect of BthTX-I may be explained by the action of this toxin into the host cells after virus entry and during virus replication, as showed by Fernard and collaborators for HIV strains inhibition [47]. The authors demonstrated that secreted PLA₂s blocked virus entry by preventing virion uncoating and dissociation of the RT complex from host cell membranes. Despite the stronger antiviral activity of PLA₂s are associated with their catalytic activity, they are not exclusively dependent on that, since PLA₂s with no catalytic activity also show potent antiviral effects [16,17], suggesting that PLA₂s may possess different mechanisms of action. As showed by Muller and collaborators, the possible explanation for the antiviral activity of PLA₂s are their direct action on virus particles, especially enveloped virus, leading to a membrane destabilization and, release of viral genome [44]. The mode of action for Asp49 PLA₂s could be directly on the membrane phospholipids of the viral envelope, via glycerophospholipid cleavage, while for Lys49 PLA₂s, could be a lipid disturbance on the envelope, since they are able to hydrolyze the outer phospholipid layer, accumulating fatty acids and lysophospholipids on the membrane, and leading to an increased permeability of the viral envelope, given that they possess no enzymatic activity [17,44,48,49]. These mechanisms of action were previously observed for other enveloped virus, such as DENV, YFV, and Rocio virus,

from the *Flaviviridae* family [16,17,44]. Therefore, additional studies are needed to characterize their specific sites of acting on ZIKV particles.

As the strongest effects observed in our data for BthTX-I and BthTX-II were in the early stages of infection, we further investigate possible binding interactions of these toxins with the ZIKV particle. A blind molecular docking analysis using both PLA₂s and the E protein of ZIKV was performed, and the protein-protein docking analyses demonstrated that BthTX-I and BthTX-II are predicted to bind to E protein in the DII and DIII domains, which corroborate to their *in vitro* virucidal effect on the ZIKV particle. The tip of DII contains the fusion loop (FL), the portion that interacts with the host membrane during membrane fusion [50], and DIII possesses the receptor-binding site, the portion of great importance during the fusion process [51], that could also explain the blockage of ZIKV entry into host cells. This potential interaction with E protein was also corroborated by the infrared spectrum data, suggesting interaction of viral surface proteins by amide III for BthTX-I and BthTX-II, and interaction with glycosylated proteins for BthTX-I. Besides, the analysis of the association of ZIKV with BthTX-II suggests the interaction with C=O vibrations and C=N vibrations to guanine in ZIKV, which may represent a potential effect on genomic RNA of ZIKV, corroborating with the findings of the activity of this toxin on the post-entry stages of ZIKV replication.

Our findings demonstrate that the PLA₂s BthTX-I and BthTX-II could be useful for the development of antiviral compounds against ZIKV infection. The virucidal activity of these proteins on ZIKV, as well as their high SI, make them as promising templates for the development of future drug candidates against Zika fever.

5. Acknowledgments

NMC and IAS thank to Conselho Nacional de Desenvolvimento Científico e Tecnológico (CNPq; scholarships # 133956/2020-2 and # 142495/2020-4, respectively). ACGJ and RSS are grateful to Coordenação de Aperfeiçoamento de Pessoal de Nível Superior (CAPES)—Brasil—Prevention and Combat of Outbreaks, Endemics, Epidemics and Pandemics—Finance Code #88881.506794/2020-01. ACGJ is also grateful to FAPEMIG (Minas Gerais Research Foundation APQ-03385-18) and CAPES—Finance Code 001.

6. References

- [1] B.H. Song, S.I. Yun, M. Woolley, Y.M. Lee, Zika virus: History, epidemiology, transmission, and clinical presentation, *J. Neuroimmunol.* 308 (2017) 50–64. <https://doi.org/10.1016/j.jneuroim.2017.03.001>.
- [2] F. Javed, K.N. Manzoor, M. Ali, I.U. Haq, A.A. Khan, A. Zaib, S. Manzoor, Zika virus: what we need to know?, *J. Basic Microbiol.* 58 (2018) 3–16. <https://doi.org/10.1002/jobm.201700398>.
- [3] A. Agrelli, R.R. de Moura, S. Crovella, L.A.C. Brandão, ZIKA virus entry mechanisms in human cells, *Infect. Genet. Evol.* 69 (2019) 22–29. <https://doi.org/10.1016/J.MEEGID.2019.01.018>.
- [4] S. Bos, W. Viranaicken, J. Turpin, C. El-Kalamouni, M. Roche, P. Krejbich-Trotot, P. Desprès, G. Gadea, The structural proteins of epidemic and historical strains of Zika virus differ in their ability to initiate viral infection in human host cells, *Virology.* 526 (2019) 233. <https://doi.org/10.1016/j.virol.2018.11.006>.
- [5] S. Masmajan, D. Musso, M. Vouga, L. Pomar, P. Dashraath, M. Stojanov, A. Panchaud, D. Baud, Zika Virus, *Pathogens.* 9 (2020). <https://doi.org/10.3390/pathogens9110898>.
- [6] B.D. Foy, K.C. Kobylinski, J.L.C. Foy, B.J. Blitvich, A.T. da Rosa, A.D. Haddow, R.S. Lanciotti, R.B. Tesh, Probable Non-Vector-borne Transmission of Zika Virus, Colorado, USA, *Emerg. Infect. Dis.* 17 (2011) 880–882. <https://doi.org/10.3201/eid1705.101939>.
- [7] M. Besnard, S. Lastère, A. Teissier, V.M. Cao-Lormeau, D. Musso, Evidence of perinatal transmission of zika virus, French Polynesia, December 2013 and February 2014, *Eurosurveillance.* 19 (2014) 20751. <https://doi.org/10.2807/1560-7917.ES2014.19.13.20751>.
- [8] M.M. Magnus, D.L.A. Espósito, V.A. da Costa, P.S. de Melo, C. Costa-Lima, B.A.L. da Fonseca, M. Addas-Carvalho, Risk of Zika virus transmission by blood donations in Brazil, *Hematol. Transfus. Cell Ther.* 40 (2018) 250–254. <https://doi.org/10.1016/j.htct.2018.01.011>.
- [9] G. Calvet, R.S. Aguiar, A.S.O. Melo, S.A. Sampaio, I. de Filippis, A. Fabri, E.S.M. Araujo, P.C. de Sequeira, M.C.L. de Mendonça, L. de Oliveira, D.A. Tschoeke, C.G. Schrago, F.L. Thompson, P. Brasil, F.B. dos Santos, R.M.R. Nogueira, A. Tanuri, A.M.B. de Filippis, Detection and sequencing of Zika virus

- from amniotic fluid of fetuses with microcephaly in Brazil: a case study, *Lancet Infect. Dis.* 16 (2016) 653–660. [https://doi.org/10.1016/S1473-3099\(16\)00095-5](https://doi.org/10.1016/S1473-3099(16)00095-5).
- [10] S. Ali, O. Gugliemini, S. Harber, A. Harrison, L. Houle, J. Ivory, S. Kersten, R. Khan, J. Kim, C. LeBoa, E. Nez-Whitfield, J. O’Marr, E. Rothenberg, R.M. Segnitz, S. Sila, A. Verwillow, M. Vogt, A. Yang, E.A. Mordecai, Environmental and Social Change Drive the Explosive Emergence of Zika Virus in the Americas, *PLoS Negl. Trop. Dis.* 11 (2017) 1–16. <https://doi.org/10.1371/journal.pntd.0005135>.
- [11] B. Rozé, F. Najioullah, J. Fergé, K. Apetse, Y. Brouste, R. Cesaire, C. Fagour, L. Fagour, P. Hochedez, S. Jeannin, J. Joux, H. Mehdaoui, R. Valentino, A. Signate, A. Cabié, Zika virus detection in urine from patients with Guillain-Barré syndrome on Martinique, January 2016, *Eurosurveillance.* 21 (2016) 8–11. <https://doi.org/10.2807/1560-7917.ES.2016.21.9.30154>.
- [12] Yakob; Laith, Zika Virus after the Public Health Emergency of International Concern Period, Brazil.pdf, *Emerg. Infect. Dis.* 28 (2022) 837–840.
- [13] P.H.A. Bezerra, I.M. Ferreira, B.T. Franceschi, F. Bianchini, L. Ambrósio, A.C.O. Cintra, S.V. Sampaio, F.A. De Castro, M.R. Torqueti, BthTX-I from *Bothrops jararacussu* induces apoptosis in human breast cancer cell lines and decreases cancer stem cell subpopulation, *J. Venom. Anim. Toxins Incl. Trop. Dis.* 25 (2019) 1–9. <https://doi.org/10.1590/1678-9199-jvatitd-2019-0010>.
- [14] L.G. Barbosa, T.R. Costa, I.P. Borges, M.S. Costa, A.C. Carneiro, B.C. Borges, M.J.B. Silva, F.G. Amorim, L. Quinton, K.A.G. Yoneyama, V. de Melo Rodrigues, S.V. Sampaio, R.S. Rodrigues, A comparative study on the leishmanicidal activity of the L-amino acid oxidases BjussuLAAO-II and BmooLAAO-II isolated from Brazilian *Bothrops* snake venoms, *Int. J. Biol. Macromol.* 167 (2021) 267–278. <https://doi.org/10.1016/j.ijbiomac.2020.11.146>.
- [15] R. De Melo Alves Paiva, R. De Freitas Figueiredo, G.A. Antonucci, H.H. Paiva, M. De Lourdes Pires Bianchi, K.C. Rodrigues, R. Lucarini, R.C. Caetano, R.C. Linhari Rodrigues Pietro, C.H. Gomes Martins, S. De Albuquerque, S.V. Sampaio, Cell cycle arrest evidence, parasiticidal and bactericidal properties induced by L-amino acid oxidase from *Bothrops atrox* snake venom, *Biochimie.* 93 (2011) 941–947. <https://doi.org/10.1016/j.biochi.2011.01.009>.
- [16] V.D.M. Muller, R.R. Russo, A.C. Oliveira Cintra, M.A. Sartim, R. De Melo Alves-Paiva, L.T.M. Figueiredo, S.V. Sampaio, V.H. Aquino, Crotoxin and

- phospholipases A 2 from *Crotalus durissus terrificus* showed antiviral activity against dengue and yellow fever viruses, *Toxicon*. 59 (2012) 507–515. <https://doi.org/10.1016/j.toxicon.2011.05.021>.
- [17] A.B. Cecilio, S. Caldas, R.A. De Oliveira, A.S.B. Santos, M. Richardson, G.B. Naumann, F.S. Schneider, V.G. Alvarenga, M.I. Estevão-Costa, A.L. Fuly, J.A. Eble, E.F. Sanchez, Molecular characterization of Lys49 and Asp49 phospholipases A₂ from snake venom and their antiviral activities against Dengue virus, *Toxins (Basel)*. 5 (2013) 1780–1798. <https://doi.org/10.3390/TOXINS5101780>.
- [18] H. Brenes, G.D. Loría, B. Lomonte, Potent virucidal activity against Flaviviridae of a group IIA phospholipase A 2 isolated from the venom of *Bothrops asper*, *Biologicals*. 63 (2020) 48–52. <https://doi.org/10.1016/J.BIOLOGICALS.2019.12.002>.
- [19] S.C. Teixeira, M.S. da Silva, A.A.S. Gomes, N.S. Moretti, D.S. Lopes, E.A.V. Ferro, V. de M. Rodrigues, Panacea within a Pandora’s box: the antiparasitic effects of phospholipases A 2 (PLA 2 s) from snake venoms, *Trends Parasitol*. 38 (2022) 80–94. <https://doi.org/10.1016/J.PT.2021.07.004>.
- [20] Y.N. Utkin, Animal venom studies: Current benefits and future developments, *World J. Biol. Chem*. 6 (2015) 28. <https://doi.org/10.4331/wjbc.v6.i2.28>.
- [21] J. Gutiérrez, B. Lomonte, Phospholipase A₂ myotoxins from *Bothrops* snake venoms, *Toxicon*. 33 (1995) 1405–1424. [https://doi.org/10.1016/0041-0101\(95\)00085-Z](https://doi.org/10.1016/0041-0101(95)00085-Z).
- [22] S.C. Teixeira, B.C. Borges, V.Q. Oliveira, L.S. Carregosa, L.A. Bastos, I.A. Santos, A.C.G. Jardim, F.F. Melo, Insights into the antiviral activity of phospholipases A 2 (PLA 2 s) from snake venoms, (2020).
- [23] I.A. Santos, J.F. Shimizu, D.M. de Oliveira, D.O.S. Martins, L. Cardoso-Sousa, A.C.O. Cintra, V.H. Aquino, S.V. Sampaio, N. Nicolau-Junior, R. Sabino-Silva, A. Merits, M. Harris, A.C.G. Jardim, Chikungunya virus entry is strongly inhibited by phospholipase A₂ isolated from the venom of *Crotalus durissus terrificus*, *Sci. Rep*. 11 (2021) 1–12. <https://doi.org/10.1038/s41598-021-88039-4>.
- [24] J.F. Shimizu, C.M. Pereira, C. Bittar, M.N. Batista, G.R.F. Campos, S. Da Silva, A.C.O. Cintra, C. Zothner, M. Harris, S.V. Sampaio, V.H. Aquino, P. Rahal, A.C.G. Jardim, Multiple effects of toxins isolated from *Crotalus durissus terrificus* on the hepatitis C virus life cycle, *PLoS One*. 12 (2017).

- <https://doi.org/10.1371/journal.pone.0187857>.
- [25] A.B. Mukherjee, L. Miele, N. Pattabiraman, Phospholipase A2 enzymes: Regulation and physiological role, *Biochem. Pharmacol.* 48 (1994) 1–10. [https://doi.org/10.1016/0006-2952\(94\)90216-X](https://doi.org/10.1016/0006-2952(94)90216-X).
- [26] S.H. Andrião-Escarso, A.M. Soares, V.M. Rodrigues, Y. Angulo, C. Díaz, B. Lomonte, J.M. Gutiérrez, J.R. Giglio, Myotoxic phospholipases A2 in Bothrops snake venoms: Effect of chemical modifications on the enzymatic and pharmacological properties of bothropstoxins from *Bothrops jararacussu*, *Biochimie.* 82 (2000) 755–763. [https://doi.org/10.1016/S0300-9084\(00\)01150-0](https://doi.org/10.1016/S0300-9084(00)01150-0).
- [27] J.M. Gutiérrez, J. Núñez, A.C.O. Cintra, M.I. Homsí-Brandeburgo, J.R. Giglio, Skeletal muscle degeneration and regeneration after injection of bothropstoxin-II, a phospholipase A2 isolated from the venom of the snake *Bothrops jararacussu*, *Exp. Mol. Pathol.* 55 (1991) 217–229. [https://doi.org/10.1016/0014-4800\(91\)90002-F](https://doi.org/10.1016/0014-4800(91)90002-F).
- [28] M.I. Homsí-Brandeburgo, L.S. Queiroz, H. Santo-Neto, L. Rodrigues-Simioni, J.R. Giglio, Fractionation of *Bothrops jararacussu* snake venom: partial chemical characterization and biological activity of bothropstoxin, *Toxicon.* 26 (1988) 615–627. [https://doi.org/10.1016/0041-0101\(88\)90244-9](https://doi.org/10.1016/0041-0101(88)90244-9).
- [29] A.C.O. Cintra, S. Marangoni, B. Oliveira, J.R. Giglio, Bothropstoxin-I: amino acid sequence and function, *J. Protein Chem.* 12 (1993) 57–64. <https://doi.org/10.1007/BF01024915>.
- [30] S. Silva, J.F. Shimizu, D.M. de Oliveira, L.R. de Assis, C. Bittar, M. Mottin, B.K. de P. Sousa, N.C. de M.R. Mesquita, L.O. Regasini, P. Rahal, G. Oliva, A.L. Perryman, S. Ekins, C.H. Andrade, L.R. Goulart, R. Sabino-Silva, A. Merits, M. Harris, A.C.G. Jardim, A diarylamine derived from anthranilic acid inhibits ZIKV replication, *Sci. Rep.* 9 (2019) 1–12. <https://doi.org/10.1038/s41598-019-54169-z>.
- [31] C.L. Donald, B. Brennan, S.L. Cumberworth, V. V. Rezelj, J.J. Clark, M.T. Cordeiro, R. Freitas de Oliveira França, L.J. Pena, G.S. Wilkie, A. Da Silva Filipe, C. Davis, J. Hughes, M. Varjak, M. Selinger, L. Zuvanov, A.M. Owsianka, A.H. Patel, J. McLauchlan, B.D. Lindenbach, G. Fall, A.A. Sall, R. Biek, J. Rehwinkel, E. Schnettler, A. Kohl, Full Genome Sequence and sRNA Interferon Antagonist Activity of Zika Virus from Recife, Brazil, *PLoS Negl. Trop. Dis.* 10 (2016) e0005048.

- <https://doi.org/10.1371/JOURNAL.PNTD.0005048>.
- [32] Y. Yan, H. Tao, J. He, S.Y. Huang, The HDock server for integrated protein–protein docking, *Nat. Protoc.* 15 (2020) 1829–1852. <https://doi.org/10.1038/S41596-020-0312-X>.
- [33] E.F. Pettersen, T.D. Goddard, C.C. Huang, G.S. Couch, D.M. Greenblatt, E.C. Meng, T.E. Ferrin, UCSF Chimera-A Visualization System for Exploratory Research and Analysis, *J Comput Chem.* 25 (2004) 1605–1612. <https://doi.org/10.1002/jcc.20084>.
- [34] R.A. Laskowski, M.B. Swindells, LigPlot+: Multiple ligand-protein interaction diagrams for drug discovery, *J. Chem. Inf. Model.* 51 (2011) 2778–2786. <https://doi.org/10.1021/ci200227u>.
- [35] A. Kohler, D. Bertrand, H. Martens, K. Hannesson, C. Kirschner, R. Ofstad, Multivariate image analysis of a set of FTIR microspectroscopy images of aged bovine muscle tissue combining image and design information, *Anal. Bioanal. Chem.* 389 (2007) 1143–1153. <https://doi.org/10.1007/S00216-007-1414-9>.
- [36] L. Rieppo, S. Saarakkala, T. Närhi, H.J. Helminen, J.S. Jurvelin, J. Rieppo, Application of second derivative spectroscopy for increasing molecular specificity of Fourier transform infrared spectroscopic imaging of articular cartilage, *Osteoarthr. Cartil.* 20 (2012) 451–459. <https://doi.org/10.1016/J.JOCA.2012.01.010>.
- [37] P.I. Haris, Probing protein-protein interaction in biomembranes using Fourier transform infrared spectroscopy, *Biochim. Biophys. Acta.* 1828 (2013) 2265–2271. <https://doi.org/10.1016/J.BBAMEM.2013.04.008>.
- [38] L. V. Bel'skaya, E.A. Sarf, D. V. Solomatin, Application of FTIR Spectroscopy for Quantitative Analysis of Blood Serum: A Preliminary Study, *Diagnostics* (Basel, Switzerland). 11 (2021). <https://doi.org/10.3390/DIAGNOSTICS11122391>.
- [39] Z. Movasaghi, S. Rehman, I.U. Rehman, Fourier Transform Infrared (FTIR) Spectroscopy of Biological Tissues, *https://doi.org/10.1080/05704920701829043*. 43 (2008) 134–179. <https://doi.org/10.1080/05704920701829043>.
- [40] A. Martinez-Cuazitl, G.J. Vazquez-Zapien, M. Sanchez-Brito, J.H. Limon-Pacheco, M. Guerrero-Ruiz, F. Garibay-Gonzalez, R.J. Delgado-Macuil, M.G.G. de Jesus, M.A. Corona-Perezgrovas, A. Pereyra-Talamantes, M.M. Mata-

- Miranda, ATR-FTIR spectrum analysis of saliva samples from COVID-19 positive patients, *Sci. Rep.* 11 (2021). <https://doi.org/10.1038/S41598-021-99529-W>.
- [41] S. Cai, B.R. Singh, Identification of beta-turn and random coil amide III infrared bands for secondary structure estimation of proteins, *Biophys. Chem.* 80 (1999) 7–20. [https://doi.org/10.1016/S0301-4622\(99\)00060-5](https://doi.org/10.1016/S0301-4622(99)00060-5).
- [42] R.M. Kini, Excitement ahead: structure, function and mechanism of snake venom phospholipase A2 enzymes, *Toxicon.* 42 (2003) 827–840. <https://doi.org/10.1016/J.TOXICON.2003.11.002>.
- [43] R.H. Schaloske, E.A. Dennis, The phospholipase A2 superfamily and its group numbering system, *Biochim. Biophys. Acta - Mol. Cell Biol. Lipids.* 1761 (2006) 1246–1259. <https://doi.org/10.1016/J.BBALIP.2006.07.011>.
- [44] V.D. Muller, R.O. Soares, N.N. Dos Santos-Junior, A.C. Trabuco, A.C. Cintra, L.T. Figueiredo, A. Caliri, S.V. Sampaio, V.H. Aquino, Phospholipase A2 isolated from the venom of *Crotalus durissus terrificus* inactivates dengue virus and other enveloped viruses by disrupting the viral envelope, *PLoS One.* 9 (2014) 1–10. <https://doi.org/10.1371/journal.pone.0112351>.
- [45] M. Mitsuishi, S. Masuda, I. Kudo, M. Murakami, Group V and X secretory phospholipase A2 prevents adenoviral infection in mammalian cells, *Biochem. J.* 393 (2006) 97–106. <https://doi.org/10.1042/BJ20050781>.
- [46] A.E. Siniavin, M.A. Streltsova, M.A. Nikiforova, · Denis, S. Kudryavtsev, S.D. Grinkina, V.A. Gushchin, V.A. Mozhaeva, V.G. Starkov, · Alexey, V. Osipov, S.C.R. Lummis, · Victor, I. Tsetlin, Y.N. Utkin, Snake venom phospholipase A2 s exhibit strong virucidal activity against SARS-CoV-2 and inhibit the viral spike glycoprotein interaction with ACE2, *Cell. Mol. Life Sci.* 78 (2021) 7777–7794. <https://doi.org/10.1007/s00018-021-03985-6>.
- [47] D. Fenard, G. Lambeau, E. Valentin, J.C. Lefebvre, M. Lazdunski, A. Doglio, Secreted phospholipases A(2), a new class of HIV inhibitors that block virus entry into host cells, *J. Clin. Invest.* 104 (1999) 611–618. <https://doi.org/10.1172/JCI6915>.
- [48] J.C. Wilschut, J. Regts, G. Scherphof, Action of phospholipase A2 on phospholipid vesicles. Preservation of the membrane permeability barrier during asymmetric bilayer degradation, *FEBS Lett.* 98 (1979) 181–186. [https://doi.org/10.1016/0014-5793\(79\)80179-9](https://doi.org/10.1016/0014-5793(79)80179-9).

- [49] J. Davidsen, O.G. Mouritsen, K. Jorgensen, Synergistic permeability enhancing effect of lysophospholipids and fatty acids on lipid membranes, *Biochim. Biophys. Acta.* 1564 (2002) 256–262. [https://doi.org/10.1016/S0005-2736\(02\)00461-3](https://doi.org/10.1016/S0005-2736(02)00461-3).
- [50] F.X. Heinz, K. Stiasny, Flaviviruses and their antigenic structure, *J. Clin. Virol.* 55 (2012) 289–295. <https://doi.org/10.1016/J.JCV.2012.08.024>.
- [51] A. Agrelli, R.R. De Moura, S. Crovella, L. André, C. Brandão, Zika virus entry mechanisms in human cells, *Infect. Genet. Evol.* (2019). <https://doi.org/10.1016/j.meegid.2019.01.018>.

Captions to Figures

Figure 1. Anti-ZIKV activity of BthTX-I and BthTX-II. Structure of the BthTX-I protein (A) and BthTX-II (B) isolated from the venom of *Bothrops jararacussu* (PDB ID: 3HZD and 2OQD, respectively). Vero E6 cells were treated with BthTX-I at concentrations ranging from 0.122 to 250 $\mu\text{g}/\text{mL}$ (C), and with BthTX-II at concentrations ranging from 0.005 ng/mL to 250 $\mu\text{g}/\text{mL}$ (D), and the effective concentration of 50% (EC_{50}) and cytotoxic concentration of 50% (CC_{50}) were determined. ZIKV replication was measured by FFU/mL (indicated by ■) and cellular viability measured using an MTT assay (indicated by ●). Mean values of three independent experiments each measured in quadruplicate including the standard deviation are shown.

Figure 2. BthTX-I and II effects on the early stages of ZIKV infection. (A) BthTX-I and BthTX-II at 12 $\mu\text{g}/\text{mL}$ and ZIKV (MOI 0.01) were simultaneously added to Vero E6 cells for 2h at 37 °C, cells were washed with PBS and replaced with fresh medium. FFU were counted 72 h.p.i. to assess ZIKV replication rates. (B) BthTX-I and BthTX-II at 12 $\mu\text{g}/\text{mL}$ and ZIKV (MOI 0.01) were incubated for 2h at 37 °C, then added to cells for extra 2h. Cells were washed with PBS, replaced with fresh medium, and FFU were counted 72 h.p.i. Schematic representation of each time-based assay as shown by Vero E6 cells (gray bars), compound (purple bars), ZIKV_{PE243} (yellow bars) and ZIKV and compounds inoculum (microtube). Mean values \pm SD of a minimum of three independent experiments each measured in quadruplicate. (****) $P < 0.0001$. All images were generated using GraphPad Prism 8.

Figure 3. Protective and post-entry activity of BthTX-I and II on ZIKV infection. (A) BthTX-I and BthTX-II at 12 $\mu\text{g}/\text{mL}$ were added to Vero E6 cells for 2h at 37 °C, cells were washed with PBS, and ZIKV_{PE243} (MOI 0,01) was added to cells for 2h at 37 °C. Cells were washed with PBS and replaced with fresh medium. FFU were counted 72 h.p.i. to assess ZIKV replication rates. (B) ZIKV_{PE243} was added to cells for 2h at 37 °C, cells were washed with PBS and then the inoculum was replaced by medium containing BthTX-I and BthTX-II. Schematic representation of time-based assay as indicated by Vero cells (gray bars), compound (purple bars) and ZIKV_{PE243} (yellow bars). Mean values \pm SD of a minimum of three independent experiments each

measured in quadruplicate. (****) $P < 0.0001$. All images were generated using GraphPad Prism 8.

Figure 4. Interaction of BthTX-I and BthTX-II with ZIKV E protein. Illustration of spatial position and the molecular docking images of the BthTX-I (blue) (PDB: 3HZD) [41] and BthTX-II (purple) (PDB: 2OQD) [42] interactions with ZIKV E protein (yellow) (PDB: 5JHM) [43]. Protein-protein complexes were generated by servidor HDOCK [30]. DI, II and III indicate the E protein domains. All images were generated using Chimera and GIMP 2.10.20.

Figure 5. Predicted molecular interactions between BthTX-I and II and ZIKV E protein. (A) 2D diagram of the interactions between ZIKV E protein amino acids (Chain A and B) in blue and BthTX-I in green (Chain C). (B) 2D diagram of the interactions between ZIKV E protein amino acids (Chain A and B) in blue and BthTX-II in green (Chain C). The dashed green line indicates hydrogen bonds, the red dashed line indicates a salt bridge and the red and magenta arcs indicate hydrophobic interactions. All images were generated using LigPlot+.

Figure 6. ATR-FTIR indicates molecular shifts in ZIKV particle induce by BthTX-I and BthTX-II. The representative infrared average spectrum of second derivative analysis from ZIKV (black line), BthTXI-I and BthTX-II (blue line representing the compounds), and each compound plus ZIKV (red line) employing a Fourier Transform Infrared (FTIR) methodology, in wavenumber ranging from 1800 to 800 cm^{-1} . A second derivative analysis, which the value heights indicate the intensity of each functional group among 1500 to 900 cm^{-1} wavenumbers (B, C, D, F, G, H, I), respectively. The second derivative spectra were created based on original data plotted in the Origin Pro 9.0 (OriginLab, Northampton, MA, USA) software and adjusted using Savitzky-Golay algorithm with polynomial order 2 and 20 points of the window.

Figures

Figure 1

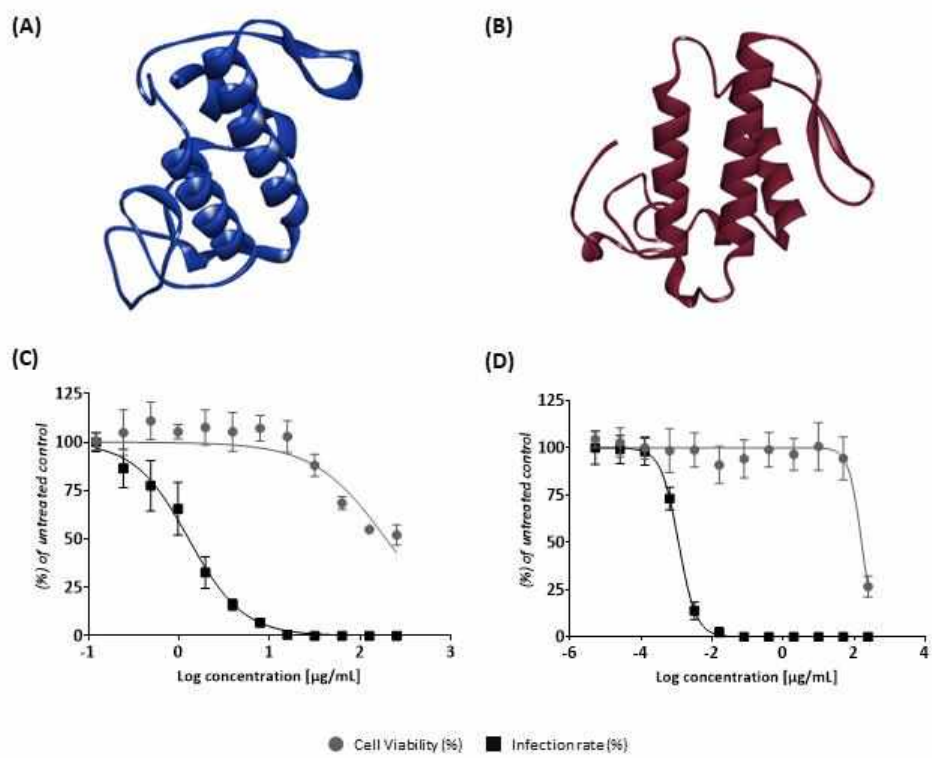


Figure 2

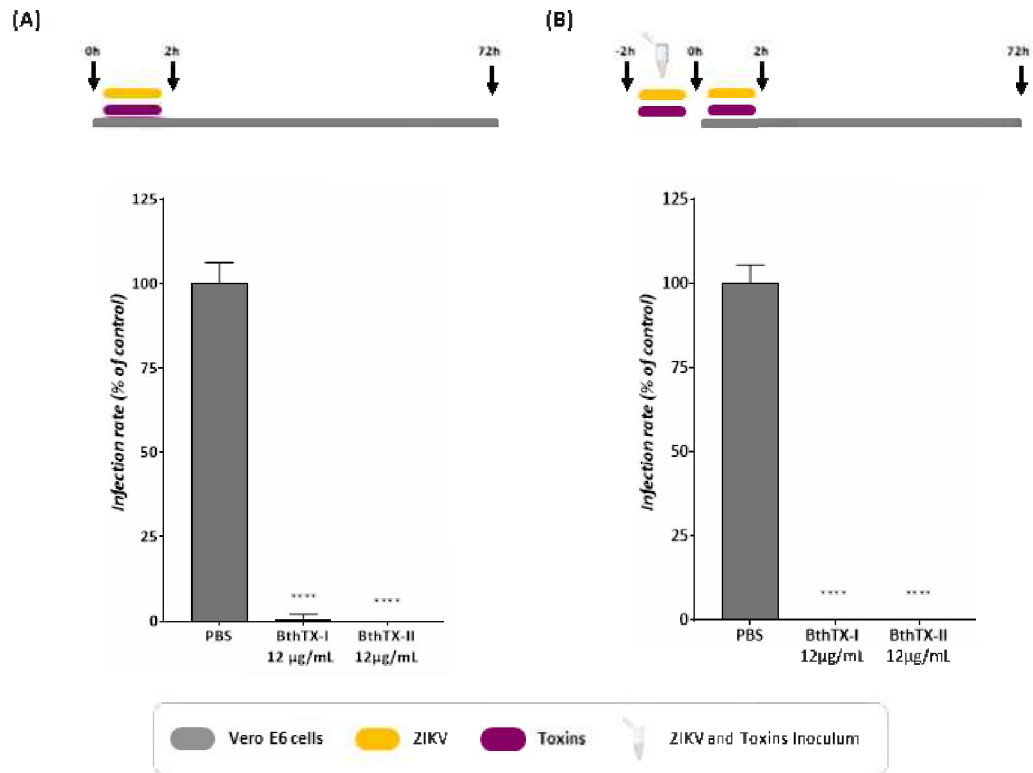


Figure 3

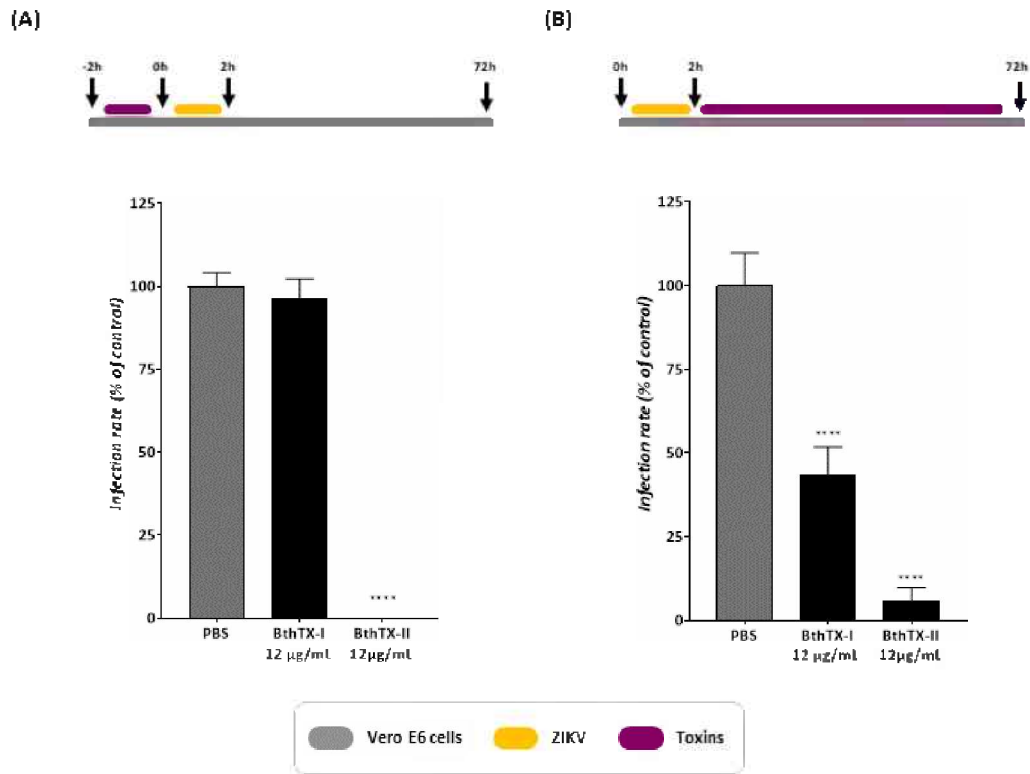


Figure 4

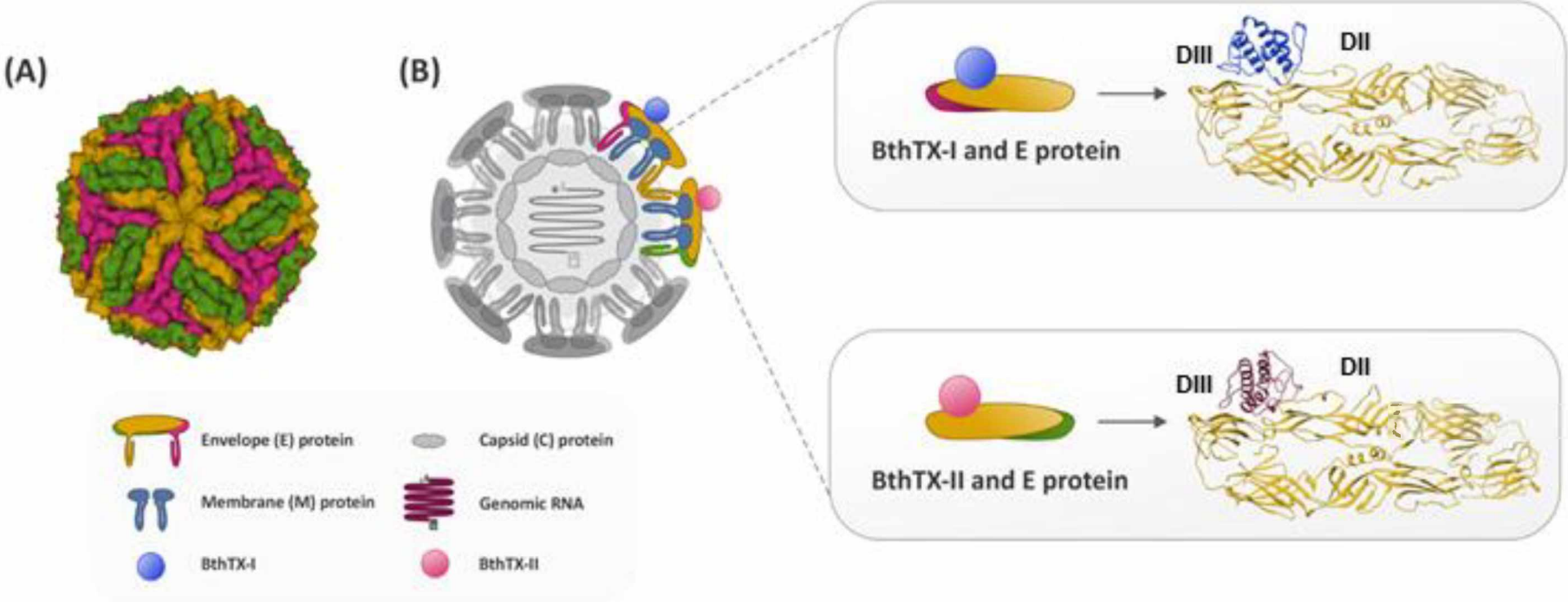
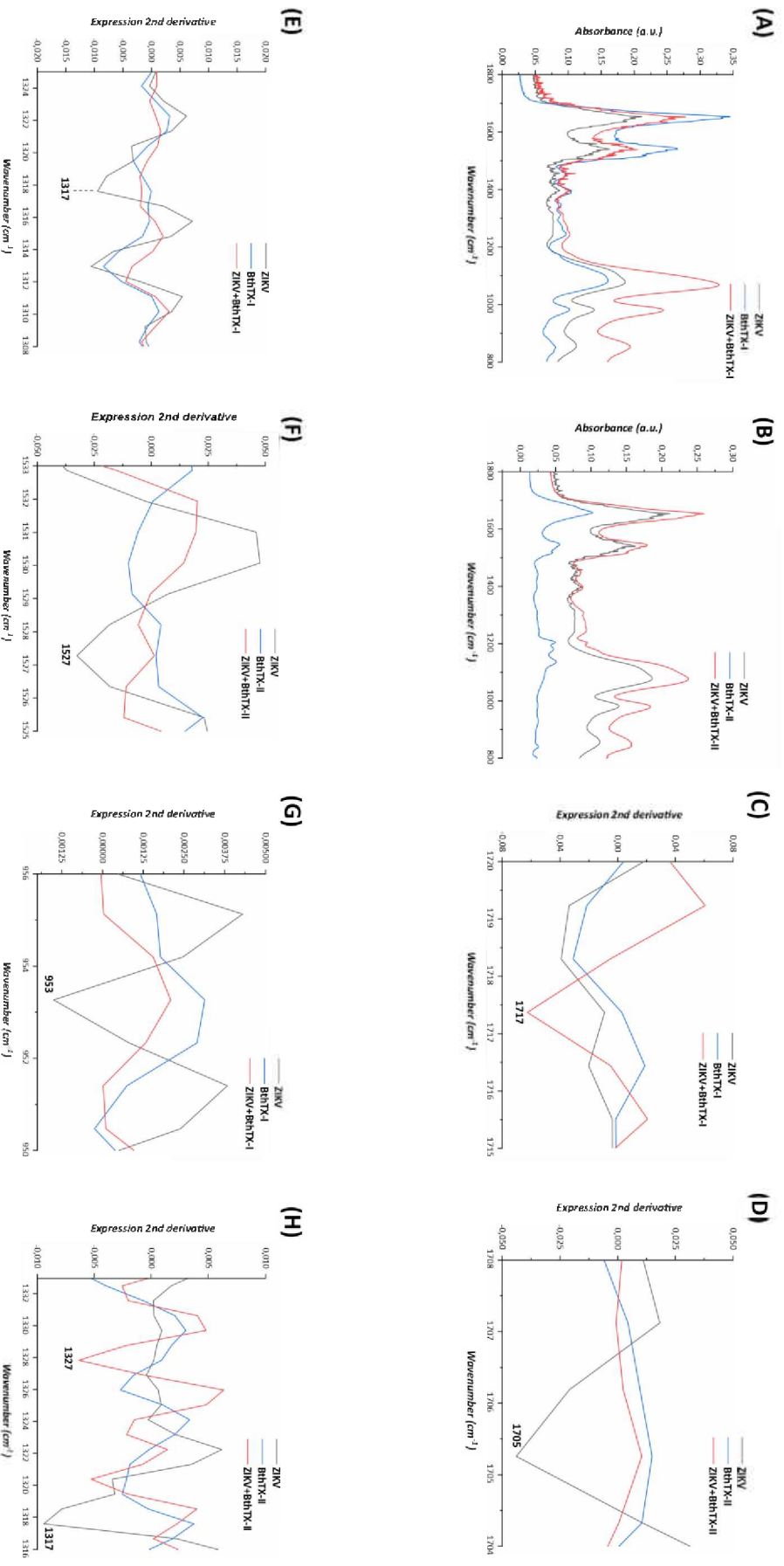


Figure 6



CAPÍTULO III

Considerações finais

Considerações finais

Os resultados deste estudo demonstram que as Bothropstoxinas I e II isoladas do veneno de *Bothrops jararacussu* (BthTX-I e BthTX-II) possuem atividade anti-ZIKV e pode servir de base para próximos estudos na busca de novos antivirais. Mais estudos são necessários para avaliar a ação antiviral desses compostos em testes *in vivo* e o estudo das vias de entrega desses compostos.

Este trabalho fornecerá informação potencial para o desenvolvimento de novas terapias antivirais.